Title : Biflavonoid as potential 3-chymotrypsin-like protease (3CLpro) inhibitor of SARS-Coronavirus

Journal Name: Result in Chemistry

Confirm co-authorship of submission to Results in Chemistry - [EMID:5d62904a70371eae]

em.rechem.0.6f22d3.cede889a@editorialmanager.com
<em.rechem.0.6f22d3.cede889a@editorialmanager.com>
on behalf of
Results in Chemistry <em@editorialmanager.com>
Fri 11/6/2020 12:41 PM

To: Yustina Sri Hartini <yustinahartini@usd.ac.id>

*This is an automated message. *

Journal: Results in Chemistry
Title: Biflavonoid as Potential 3-Chymotrypsine-like Protease (3CLpro) Inhibitor of SARS-Coronavirus
Corresponding Author: Dr Maywan Hariono
Co-Authors: Yustina Sri Hartini; Bakti Wahyu Saputra; Bryan Afela Wahono; Zerlinda Clara Auw; Friska Dwi Indayani; Lintang Adelya; Gabriel Aprilyan Sibata Namba
Manuscript Number:

Dear Yustina Sri Hartini,

Dr Maywan Hariono submitted this manuscript via Elsevier's online submission system, Editorial Manager, and you have been listed as a Co-Author of this submission.
Elsevier asks Co-Authors to confirm their consent to be listed as Co-Author and track the papers status.
In order to confirm your connection to this submission, please click here to confirm your co-authorship:

https://www.editorialmanager.com/rechem/l.asp?i=22111&l=L0WOG88A

If you have not yet registered for the journal on Editorial Manager, you will need to create an account to complete this confirmation. Once your account is set up and you have confirmed your status as Co-Author of the submission, you will be able to view and track the status of the submission as it goes through the editorial process by logging in at https://www.editorialmanager.com/rechem/
If you did not co-author this submission, please contact the Corresponding Author directly at mhariono@usd.ac.id

Thank you,

Results in Chemistry

More information and support
FAQ: What is Editorial Manager Co-Author registration?
https://service.elsevier.com/app/answers/detail/a_id/28460/supporthub/publishing/kw/co-author+editorial+manager/
%CUSTOM_AUTHORSUPPORT%
%CUSTOM_GENERALSUPPORT%

Biflavonoid as Potential 3-Chymotrypsine-like Protease (3CLpro) Inhibitor of SARS-Coronavirus

Yustina Sri Hartini, Bakti Wahyu Saputra, Bryan Afela Wahono, Zerlinda Clara, Friska Dwi Indayani, Lintang Adelya, Gabriel Aprilyan Sibata Namba and Maywan Hariono*

Faculty of Pharmacy, Sanata Dharma University, Campus III, Paingan, Maguwoharjo, Depok, Sleman 55282, Yogyakarta, Indonesia

Abstract

3CL protease is one of the key proteins expressed by SARS-Coronavirus-2 cell, the potential to be targeted in the discovery of antivirus during this COVID-19 pandemic. This protein regulates the proteolysis of viral polypeptide essential in forming RNA virus. 3CL protease was commonly targeted in the previous SARS-Coronavirus including bat and MERS, hence, by blocking this protein activity, the coronavirus should be eradicated. This study aims to review the potency of biflavonoid as the SARS-Coronovirus-2 3CL protease (3CLpro) inhibitor. The review was initiated by describing the chemical structure of biflavonoid and followed by listing its natural source. Instead, the synthetic pathway of biflavonoid was also elaborated. The 3CLpro structure and its function was also illustrated follwed by the list of its 3D-crystal structure available in protein data bank. Lastly, the pharmacophores of biflavonoid have been identifiead as protease inhibitor was also discussed. This review hopefully will help researchers to obtain a packed information about biflavonoid which could lead to the study in designing and discovering a novel SARS-Coronavirus-2 drug by targetting 3CLpro enzyme.

1. Introduction

The pandemic Covid-19 has been extending for almost 10 months since it was outbreak in January 2020 [1]. The statistic up to now (24 October 2020) is 43 M cases, 29 M recovered and 1.15 M

death, across the world. United State of America is so far a country with the highest cases as reported approximately 8.5 M [2]. Meanwhile, Indonesia is still having an increased cases that today, it has been approximately 393,000 cases with 318,000 recovered and 13,500 death [3]. This situation has made very huge impacts in all aspects of live including economy, politics, social, culture, health and education. For example, United Nations Industrial Development Organization (UNIDO) reported that since April 2020, the high income countries (30 countries) have 18% average economic losses, whereas the upper middle-income countries (13 countries) suffer 24% average losses. The lower middle-income countries (6 countries) are hurted by 22% average loss, confirming the economic crisis unleashed by the pandemic, regardless of income level [4]. The SARS-Coronavirus-2 viral vector is still debating, however, there is either bat or snake believed as the first virus transmiting species to human [5].

As some other corona viruses, SARS-CoV-2 is also a family of coronaviridae, which genomicaly composed by the structural as well as non-structural proteins. This is RNA virus in which on one hand, the structural protein contains S protein (spike), M protein (membrane), E protein (envelope) and N protein (nucleocapside) [6]. On the other hand, the non-structural protein (NSP) is an open reading frame consisting of NSP1-16 [7]. Upon entry into the host cell, the incoming viral genome is translated to produce two large precursor polyproteins 1a (pp1a) and 1ab (pp1ab) that are processed by open reading frame (ORF) 1a-encoded viral proteinases, papain-like proteinase (PLpro) and 3C-like proteinase (3CLpro), into 16 mature nonstructural proteins (NSP1–NSP16, numbered according to their order from the N-terminus to the C-terminus of the ORF 1 polyproteins). Many of the NSPs perform essential functions in viral RNA replication and transcription [8]. The virus life cycle is illustrated in Figure 1.

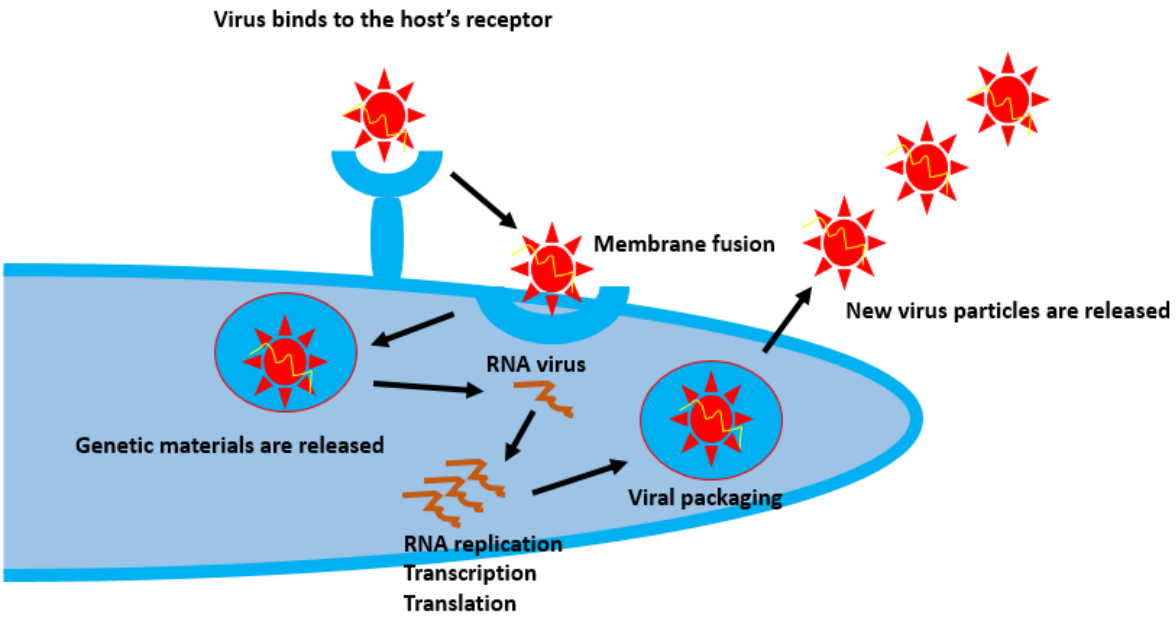

Figure 1. The life cycle of coronaviruses is initiated by the binding of the viral cell through its protein spike (S) to the host cell's receptor namely angiotensin converting enzyme 2 (ACE2). Upon membrane fusion (endocytosis), the virus is coated by endosome. The following endosomal break down releases RNA from the virus into the host cell. The incoming viral genome is translated to produce two large precursor polyproteins 1a (pp1a) and 1ab (pp1ab) which are cleaved by proteases into small products. A series of subgenomic mRNA are transcripted and finally translatted into viral proteins. The viral protein along with RNA are packed into virion in the ER and golgi and then transported via vesicles and released out of the cell [9].

One of the common studied NSPs is NSP5 in which chymotrypsin like protease (3CLpro) is one kind of this non-structural protein [10]. 3CLpro cleaves the polyprotein into viral RNA which is then replicated and packed in the new mature virus. Therefore, by interfering this proteolytic step, the viral RNA replication will be interupted leading to the prevention of new viruses for further expansion. 3CLpro is one of interesting protein targets in combating coronavirus by competitive inhibition with the peptide substrate [11].

Review on natural product compounds potential for SARS-Coronavirus have been published by targetting diverse proteins. These includes tanshinones, diarylheptanoids and geranylated flavonoids targeting PLpro [12], quercetine (reverse transcriptase) [13], aloeemodin and hesperitin (3CLpro) [14], apigenin (viral internal ribosome entry) [15], isatisindigotica (protease) [16],

amentoflavone (biflavonoid; protease) [17], kaempferol (3a ion channel) [18], glycyrrhizin (protease) [19], tetradrine (viral S and N) [20], silvestrol (cap-dependent viral mRNA translation) [21,22], etc.

Biflavonoid is currently attractive to be proposed as the serine protease inhibitor due to the suitability of its chemical structure with the active site of the protease [23]. Serine proteases are characterised by a distinctive structure, consisting of two beta-barrel domains that converge at the catalytic active site. These enzymes can be further categorised based on their substrate specificity as either trypsin-like, chymotrypsin-like or elastase-like. Therefore, the dimer form of biflavonoid is such a good inhibitor model that would fully occupy the two beta-barrel domain (main site and prime site) [24].

In this review, we will focus on the biflavonoid as the interesting compound, potential for 3CLpro inhibitor of SARS-Coronavirus-2. The review will be started by defining the chemical structure of biflavonid and its sources from both natural product as well as synthesis. The following section would be elaborating the 3CLpro structure and its function as the interesting protein target for biflavonoid. The review also summarized the available SARS-Coronavirus-2 3CLpro 3D crystal structure in protein data bank. Last but not least, the current study of the biflavonoid as a diverse protease inhibitor would be carried out to give the insight mechanism on how the biflavonoid can act as a potential SARS-CoV-2 antiviral agent.

2. Chemical structure

Biflavonoid is a natural product compound bearing a dimer of two sets of flavonoid, linked by either C-C or C-O bond [25,26]. The flavonoid itself is chemically constructed by 15-C skeleton, which is divided into two aromatic rings (Ring A and Ring B) and connected by a heterocyclic ring having α, β- unsaturated carbonyl chain [27]. Instead of flavonoid is the major form of such compound class, there are two kind analogs which enrich the flavonoid structural diversity. They are isoflavonoid (derived from 3-phenylchromen-4-one (3-phenyl-1,4-benzopyrone) and neoflavonoid (derived from 4-phenylcoumarine (4-phenyl-1,2-benzopyrone). Other subgroup of flavonoid including flavan, flavanone, flavanonol, anthocyanidin and anthoxantin are also widely distributed among natural resources [28]. Figure 2 illustrates the structure of flavonoid and its analogs.

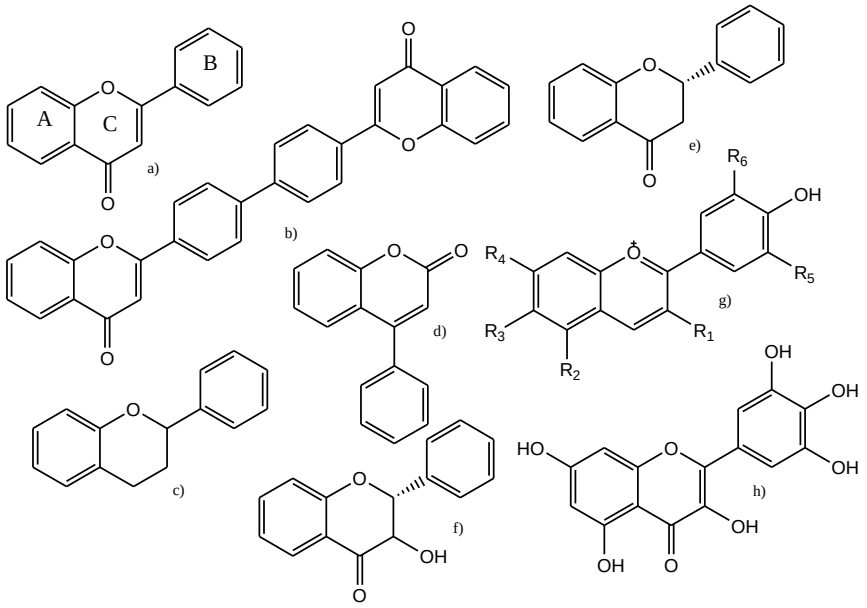

Figure 2. The structures of a) flavonoid, b) biflavonoid, c) isoflavonoid, d) neoflavonoid, e) flavanone, f) flavanonol, g) anthocyanidin and h) anthoxantin which are naturally occured in plants.

The aromatic rings are often decorated by poly-hydroxy group, therefore this compound's class are frequently called polyphenolic compounds. The presence of OH group also has a chance for the flavonoid to be biosyntheticaly formed in a glycoside. The sugar moiety in the glycosidic form makes the flavonoid more soluble in water than organic solvents, due to the polar character of the sugar [29,30].

Spectroscopically, alike to polyphenolic flavonoid, the yellowish biflavonoid absorbs UV light at 500-600 nm. The colorimetric reaction namely batochromic shift (red shift) occurs when it reacts with alkaline solution to prolong the maximum wavelength (650 nm). Vice versa, polyvalent ion such as Al^{3+} may shift the wavelength into hypsochromic shift (blue shift) with a lower wavelength (450 nm) [31]. Using fourier transform infrared (FTIR) spectroscopy, the carbonyl of chromone group stretching vibration is transmitted at 1600 cm^{-1}, meanwhile the vinyl aromatic group appears at 3600 cm^{-1} as a bending vibration [32]. The proton of biflavonoid is indicated as multiplet signals around 6-8 ppm which often overlap in *trans*/ *cis* configuration protons of α, β- unsaturated carbonyl chain as confirmed by nuclear magnetic resonance (NMR) spectroscopy. In conjunction, the carbon signal of carbonyl chromone group is indicated in 160 ppm, whereas the vinylic aromatic carbon appears at 150 ppm. Using mass spectroscopy, the origin of flavonoid sceleton

could be the most stable mass/ ion (base peak) during the fragmentation due to electron impact bombardment [33].

3. Natural sources

A naturally occuring biflavonoid is distributed in various plant species. The first isolated natural biflavonoid was from *Ochna squarrosa* Linn. (Ochnaceae) [34], and later was from *Lonicera japonica* (Caprifoliaceae) [35]. *Torreya nucifera* was also identified as the natural source producing four biflavonoids [36]. Amentoflavone is another kind of biflavonoid isolated from abroad family of plants such as selaginellaceae, cupressaceae, euphorbiaceae, podocarpaceae, and calophyllaceae [37]. It was reported for at least 127 biflavonoids distributed among plants, but the most occurences are *Gingko biloba*, *Lobelia chinensis*, *Polygala sibirica*, *Ranunculus ternatus*, *Selaginella pulvinata*, *Selagenella tamariscina* [37].

More recent study had identified the biflavonoid I3′,II8-binaringenin in drupes of *Schinus terebinthifolius*, was indicated by UHPLC-MS [38]. Five biflavonoids was lately found in *Ceratodon purpureus* presenting a diastereomerism in the second biflavonoid [39]. In the same year, three biflavonoid type were also discovered in *Selaginella doederleinii* including amentoflavone type, robustaflavone type, and hinokiflavone type [40]. From the family of zingiberaceae, new biflavonoids with flavanone-chalcone type existing in fingerroot (*Boesenbergia rotunda*) [41]. The pure biflavonoid with aglycones morelloflavone (Mo) type, volkensiflavone (Vo) type , as well as the morelloflavone's glycoside fukugiside (Fu) type were characterized in *Garcinia madruno* [42]. The genus of garcinia again was shown its resource of biflavonoid by discovering seven compounds including volkensiflavone, fukugetin, fukugeside, GB 1a, GB 1a glucoside, GB 2a, and GB 2a glucoside from *Garcinia xanthochymus* fruits [43]. Figure 3 illustrates the chemical structure of hinokiflavone, ochnaflavone, morelloflavone and volkensiflavone. For more data, Table 1 tabulates the various study reporting biflavonid found in natural source in the last three years.

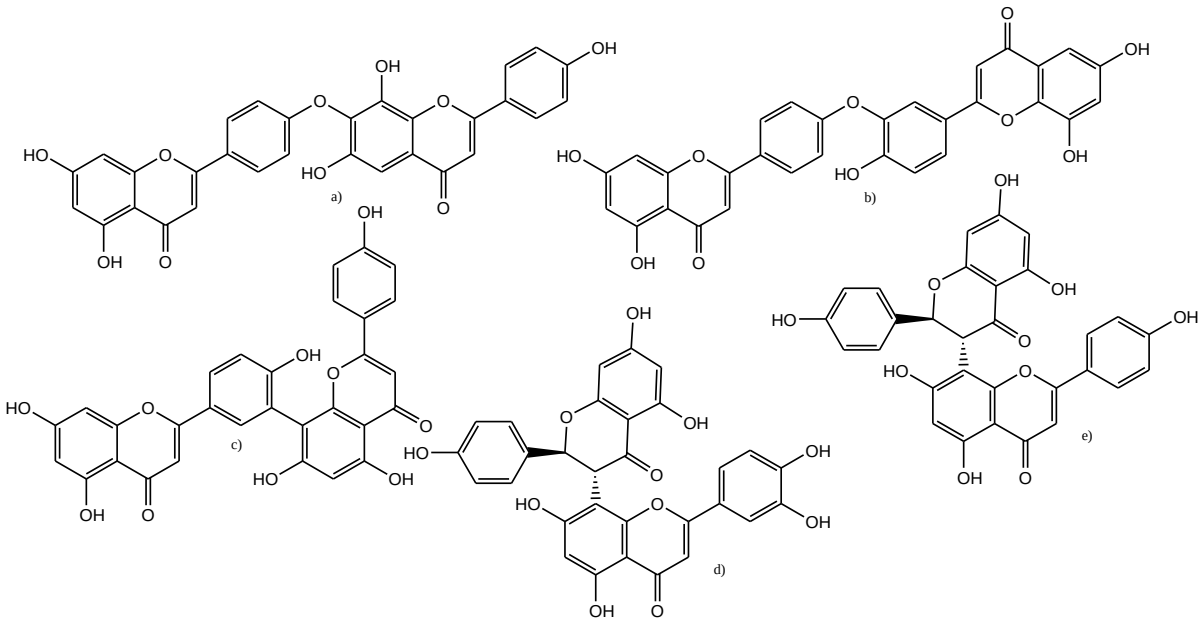

Figure 3. The chemical structures of earlier biflavonoid found in plants: a) hinokiflavone, b) ochnaflavone, c) amentoflavone, d) morelloflavone, and e) volkensiflavone.

Table 1. Biflavonoids from natural resources have been reported in the last three years.

No	Biflavonoid	Plants	References
1	dihydrodaphnodorin B	*Fumana procumbens*	[44]
2	daphnodorin B	*Fumana procumbens*	[44]
3	volkesiflavone	*Garcinia gardneriana*	[45]
4	morelloflavone	*Garcinia gardneriana, Garcinia madruno*	[45]
5	7,7″-di-*O*-methylchamaejasmin	*Ormocarpum kirkii*	[46]
6	campylospermone A	*Ormocarpum kirkii*	[46]
7	a dimeric chromene [diphysin	*Ormocarpum kirkii*	[46]
8	amentoflavone 7″-*O*-*β*-*d*-glucopyranoside	*Ginkgo Biloba*	[47]
9	bilobetin	*Ginkgo Biloba*	[47]
10	isoginkgetin	*Ginkgo Biloba*	[47]
11	sciadopitysin	*Ginkgo Biloba*	[48]
12	agathisflavone	*Schinus terebinthifolius; Anacardium occidentale*	[49,50]
13	tetrahydroamentoflavone	*Schinus terebinthifolius*	[49]
14		*Selaginella uncinata*	[50]
15	7, 4′, 7‴, 4‴-tetra-*O*-methyl amentoflavone	*Cephalotaxus harringtonia*	[51]
16	7, 4′, 7″-tri-*O*-methyl amentoflavone	*Cephalotaxus harringtonia*	[51]
17	sequoiaflavone	*Cephalotaxus harringtonia; Ouratea ferruginea*	[51, 52]
18	amentoflavone monomethoxy derivatives		[53]
19	dihydrochalcone flavanone	*Sophora flavescens*	[54]
20	2',3'-dihydroochnaflavone	*Ochna mauritiana*	[55]
21	dulcisbiflavonoid B	*Garcinia dulcis*	[56]

22	dulcisbiflavonoid C	*Garcinia dulcis*	[56]
23	umcephabiflovin A	*Cephalotaxus oliveri*	[57]
24	umcephabiflovin B	*Cephalotaxus oliveri*	[57]
25	S-taiwanhomoflavone-B	*Cephalotaxus oliveri*	[57]
26	5, 6, 6'-trihydroxy-[1,1'-biphenyl]-3,3'-dicarboxylic acid	*M. ferrea*	[58]
27	fukugiside	*Garcinia madruno*	[59]
28	neochamaejasmin B	*Stellera chamaejasme*	[60]
29	oliveriflavone A, B, and C	*Cephalotaxus oliveri*	[61]
30	rhusflavanone	*Mesua ferrea*	[62]
31	mesuaferrone B	*Mesua ferrea*	[62]
35	sinodiflavonoids A	*Sinopodophyllum emodi*	[63]
36	sinodiflavonoids B	*Sinopodophyllum emodi*	[63]
37	oxytrodiflavanone A	*Oxytropis chiliophylla*	[64]
38	oxytrochalcoflavanones A	*Oxytropis chiliophylla*	[64]
39	oxytrochalcoflavanones B	*Oxytropis chiliophylla*	[64]
40	hinokiflavone	*Selaginella sinensis*	[65]
41	isocampylospermone A	*Ochna Serrulata*	[66]
42	campylospermone A	*Ochna Serrulata*	[66]
43	cupressuflavone	*Cupressus sempervirens*	[67]
44	(8-hydroxy-3'-*β*-*D*-galactosyl-isoflavone)-2'-8''-(4'''-hydroxy-flavone)-biflavone	*Solanum nigrum*	[68]
45	2',3',5-trihydroxy-5''-methoxy-3''-*O*- α-glucosyl-3-4'''-*O*-biflavone	*Solanum nigrum*	[68]
46	7′-*O*-methyl hinokiflavone	*Selaginella tamariscina*	[69]
47	(2*R*,3*S*)-volkensiflavone-7-*O*-*β*-acetylglucopyranoside	*Allanblackia floribunda*	[70]
48	(2*S*,3*S*)-morelloflavone-7-*O*-β-acetylglucopyranoside	*Allanblackia floribunda*	[70]
49	(*S*)-2″*R*,3″*R*- and (*R*)-2″*S*,3″*S*-dihydro-3″-hydroxyamentoflavone-7- methyl ether	*Cardiocrinum giganteum*	[71]
50	(*S*)-2″*R*,3″*R*- and (*R*)-2″*S*,3″*S*-dihydro-3″-hydroxyamentoflavone	*Cardiocrinum giganteum*	[71]
51	4,4′,7-tri-*O*-methylisocampylospermone A	*Ochna serrulata*	[72]
52	4‴-de-*O*-methylafzelone A	*Ochna serrulata*	[72]
53	serrulone A	*Ochna serrulata*	[72]
54	sumaflavone	*Juniperus phoenicea*	[73]

4. Synthetic sources

Instead of natural sources, biflavonoid is also produced via synthetic pathway. This usually aims to derivatize the biflavonoid lead compound into a modified diverse functional group could be responsible for its biological activity. In addition, the synthetic pathway could be more reproducible than isolating the biflavonoid from its genuine natural sources. This will proportionally reduce the cost of production as well as increase the yields [74,75].

Biflavonoid is synthetically formed by two units (monomer) of flavonoid underwent the Ullmann coupling reaction [76]. This reaction forms diaryl ether link between two units of flavonoid, which is conditioned by mixing them with an alkaline carbonate solution, *N*, *N*-dimethylacetamide and dry toluene solvent under nitrogen exposure, followed by heating the mixture above 100^0C for several hours [77]. The total synthesis of biflavonid is initiated by reacting *ortho*-hydroxy acetophenone with benzaldehyde under Claissen Smith condensation to form chalcone as the intermediate compound [78]. The next step is the synthesis of flavone (monomer) by iodinating the chalcone using DMSO as the solvent [79]. The detail total synthesis of biflavonoid is schemed out in Scheme 1.

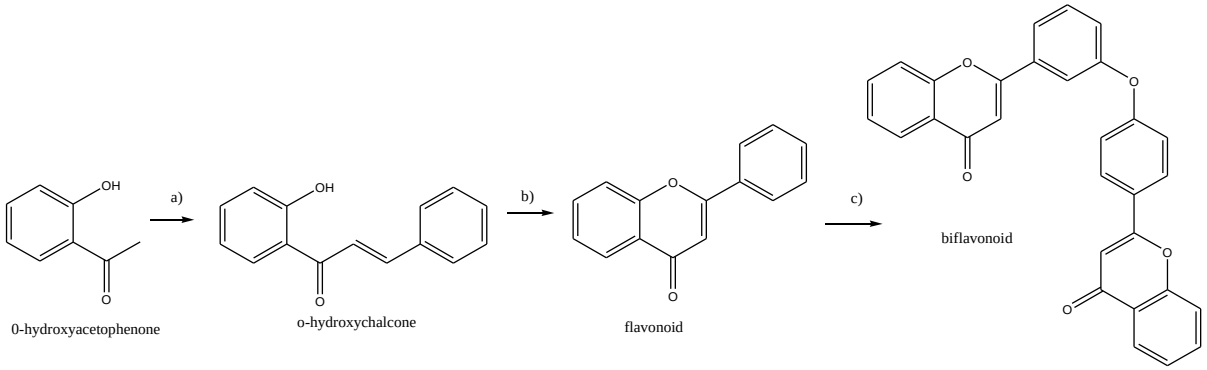

Scheme 1. Total synthesis of biflavonoid. Reagents and conditions: a) benzaldehyde, KOH, MeOH, rt, overnight, 70-87%; b) I_2, DMSO, 100 ^{o}C, overnight, 75-86%; and c) Ullmann modified coupling reaction, 8-58% [80].

An interesting biflavonoid was constructed according to naringenin monomer by reacting the available phloroglucinol and 4-hydroxy- or 4-methoxybenzaldehyde. Naringenin is the flavanone-skeleton structure attached by three hydroxy groups at the 4', 5, and 7 carbons. The product was confirmed as 3′,3‴-binaringenin and four related biflavonoids with a considerably good yield (15-35%) [81].

Biflavonoid was also prepared electrochemically by reacting flavonol isorhamnetin, $LiClO_4$ and amine in acetonitrile solvent. The mixture was electrolyzed in a diaphragm cell at anodic current density 5 mA/cm2 for 3.5 h. A platinum plate with working surface 2 cm^2 was used as the anode. Once the electrolysis completted, about 90% of the acetonitrile was distilled from the anode compartment. Further purification using chromatography column was applied and followed by recrystallization to obtain the biflavonoid product with a good yield (60-70%) [82].

A step-economical preparation of a very rare biflavonoid has been performed by combining the methylated biaurone underwent a modular and divergent synthesis strategy. The divergent synthesis was carried out by using bialdehyde as the building block such as isophthalaldehyde, terephthalaldehyde, and benzene-1,3,5-tricarbaldehyde to produce the chalcone intermediate under Claissen Smith condensation. The following reaction was oxidative cyclization to obtain the biflavonoid as the targetted compound. Interestingly, instead of biflavonoid, the divergent method ia also applied in the production triflavonoid [83].

The synthesis of biflavonoid was further explored by applying Suzuki-Miyaura cross-coupling reaction followed by alcohol methylation for the synthesis of rare 'hybrid' derivatives. These derivatives belong to different subclasses of monomers. The second biflavonoid was constructed as homodimeric compounds in which a methylenedioxy group acts as the linker between the two flavonoid monomers. This reaction facilitates the probing of uncharted regions of biologically interesting chemical space [84].

The first stereodivergent synthesis of biflavanone was conducted by exclusively controlling the temperature to produce a stereoselective product. The scaffold of 2,2'-biflavanones attached by diverse substitution at the phenyl ring and conditioned by SmI_2/ Methanol/ THF, confirmed a good yield with a high selective for both stereoisomers of the expected compounds. On one hand, the (R*,R*)-stereoisomer only formed when the temperature was controlled at -40 ^{o}C, on the other hand, the reaction generated the (R*,S*)-isomer when the mixture was refluxed [85]. The control of regioselective reaction was performed using aromatic prenyltransferase from *Aspergillus terreus* (AtaPT). Prenylation was applied to produce biflavonoids 1–3 dimerized connected by a diphenyl linkage at the hydrogen bond involving C5''–OH group. This OH is chemically less accesible than other OH groups in the ring. The AtaPT was used as the substrate that succesfully yielded the different regio and chemoselective products. This study would be recommended for developing green synthetic reactions for such prenylated biflavonoids [86].

5. 3-Chymotrypsine-like Protease

The extensive process of proteolysis releases the functional polypeptides which is mainly achieved by main proteinase and frequently also named 3C-like proteinase (3CLpro). This indicates the similar cleavage site with the early picornavirus 3C proteinases (3Cpro), although further study showed that similarity is limited by two family of the protease. 3CLpro cleaves at least 11

conserved amino acid residues includes GLN---(SER, ALA, GLY) sequences (the cleavagesite is indicated by ---) [87]. This process is initiated by the autocleavage of its own enzyme from two polypeptides (polypeptide A and polypeptide B). There are three non-canonical 3CLpro cleavage sites at the P2 position employing PHE, MET or VAL residues in SARS-Coronavirus polyproteins. The cleavage site of 3CLpro SARS-Coronavirus is illustrated in Figure 4 [88,89].

3CLpro Cleavage Site	P6	P5	P4	P3	P2	P1	P1′	P2′	P3′	P4′	P5′	Relative Kcal/Km
nsp4/5	T	S	A	V	L	Q	S	G	F	R	K	100%
nsp5/6	S	G	V	T	F	Q	G	K	F	K	K	41%
nsp6/7	K	V	A	T	V	Q	S	K	M	S	D	3%
nsp7/8	N	R	A	T	L	Q	A	I	A	S	E	5%
nsp8/9	S	A	V	K	L	Q	N	N	E	L	S	2%
nsp9/10	A	T	V	R	L	Q	A	G	N	A	T	22%
nsp10-12	R	E	P	L	M	Q	S	A	D	A	S	0,2%
nsp12/13	P	H	T	V	L	Q	A	V	G	A	C	8%
nsp13/14	N	V	A	T	L	Q	A	E	N	V	T	9%
nsp14/15	T	F	T	R	L	Q	S	L	E	N	V	28%
nsp16/15	F	Y	P	K	L	Q	A	S	Q	A	W	27%

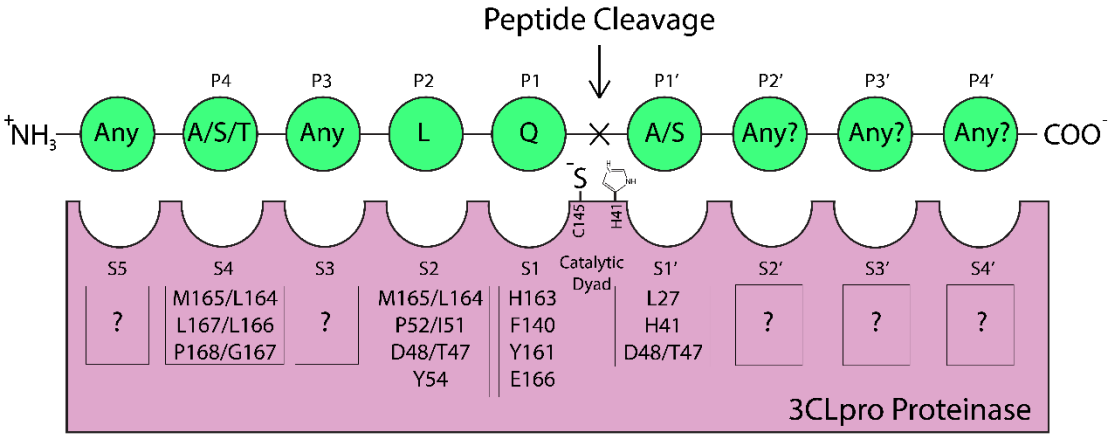

Figure 4. The 3CLpro cleavage sites of SARS CoV which recognize 11 sequences of peptide substrate with their respective Kcal/Km. This Kcal/Km values reflect the canonical recognition which is supported by the recognition sites of a series of other coronavirus 3C proteases [90,91].

The availability of experimentally determined three dimensional (3D) structures of the SARS-Coronavirus-2 3CLpro has greatly aided in the design of anti-SARS-Coronavirus-2 drug [92].

Recently, the sudden increase in the number of crystal structures of 3CLpro are deposited in the protein data bank (PDB) [93]. Most of the earlier crystal structures are devoid of inhibitor. Thus, it could not explain properly the particular binding site of 3CLpro [94]. Therefore, many earlier efforts to understand the structure and function of NS3pro relied mainly on the models developed based on the crystal structures of other betacoronavirus such as SARS-Coronavirus, MERS, Bat Corona, etc [95].

To date, there are more than 100 3D structures of SARS-Coronavirus-2 3CLpro deposited in the protein data bank (PDB) (www.rcsb.org). In general, the crystal structures 3CLpro reveal the presence of three structural domains in each monomer wherein domains I (position 8-101), II (position 102-184) and III (position 201-303) has a characteristic chymotrypsin-like fold with a catalytic cysteine (CYS145) and histidine (HIS41). This is linked to a third C-terminal domain by a long loop (position 185-200) by orienting the N-terminal residues that are essential for the dimerization [96-99]. Domain I and domain II are decorated in an antiparallel β-barrel structure, whereas the domain III is composed by five α-helices arranged in a globular cluster. The helical domains of the two monomers form a dimer through H-bond interactions from end to end of the N-terminal residues and the key residues from the individual monomers. The catalytic activity is suggested to be contributed by the salt bridge between the N-terminal SER1 of one monomer and GLU166 of the other monomer [98,100]. Table 2 presenting for 115 3D-structures of 3CLpro available in protein data bank.

SARS-Coronavirus-2 3CL pro in complex with a novel inhibitor 5,6,7-trihydroxy-2-phenyl-4H-chromen-4-one was solved its 3D-crystal strucure in 2.20 Å of resolution. This flavonoid inhibitor binds to the active site of the protease through the hydrogen bond interaction between ortho-hydroxyphenyl (ring A) of the ligand with GLY143, and the carbonyl group of ring C with GLU166. The non-bonding interaction was also observed between the phenyl of ring B with HIS41 and CYS44. This complex is one of the proofs that flavonoid is such an important feature for 3CLpro pharmacophore, therefore so do the biflavonoid which could cover more space to interact with the 3CLpro. Figure 5 illustrates the interaction between 5,6,7-trihydroxy-2-phenyl-4H-chromen-4-one and the active site of SARS-Coronavirus-2 3CLpro (PDB ID 6M2N) [101].

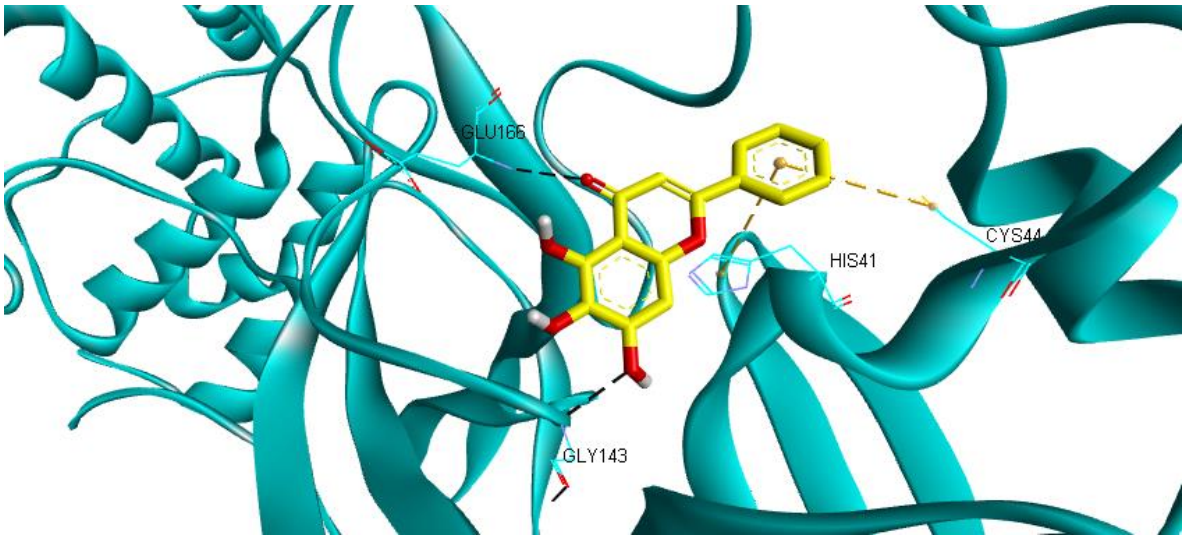

Figure 5. The interaction between 5,6,7-trihydroxy-2-phenyl-4H-chromen-4-one and the active site of SARS-Coronavirus-2 (PDB ID 6M2N). The 3CLpro is presented in a blue ribbon model, whereas the inhibitor is in a stick model (yellow = C, white = H, and red = O). The H-bond and hydrophobic interactions are presented in black and yellow dot lines, respectively.

Two peptidomimetic-based inhibitors are complexed with SARS-Coronavirus-2 in different monomer of trimer with 2.15Å of the crystal resolution (PDB 6WTT) [102]. (1*S*,2*S*)-2-({*N*-[(benzyloxy)carbonyl]-*L*-leucyl}amino)-1-hydroxy-3-[(3*S*)-2-oxopyrrolidin-3-yl]propane-1-sulfonic acid binds to the active site in the monomer A, by interacting with CYS145, GLU166, GLN189, HIS164, and PHE140 at the respective atoms of O (OH), O (C=O), H (NH-amide), H (NH-amide), and H (NH-pyrolidinone) (Figure 6). Monomer B demonstrates the same binding mode with the monomer A, whereas the monomer C is bound by *N*~2~-[(benzyloxy)carbonyl]-*N*-[(1*R*,2*S*)-1-hydroxy-3-[(3S)-2-oxopyrrolidin-3-yl]-1-(trimethyl-lambda~4~-sulfanyl)propan-2-yl]-*L*-leucinamide. In the monomer C, the ligand interacts with GLU166, HIS164, HIS41, and GLN189 at the respective atoms of O (C=O), N (NH-amide) and N- (NH-pyrilidinone), O (OH), and N (NH-amide).

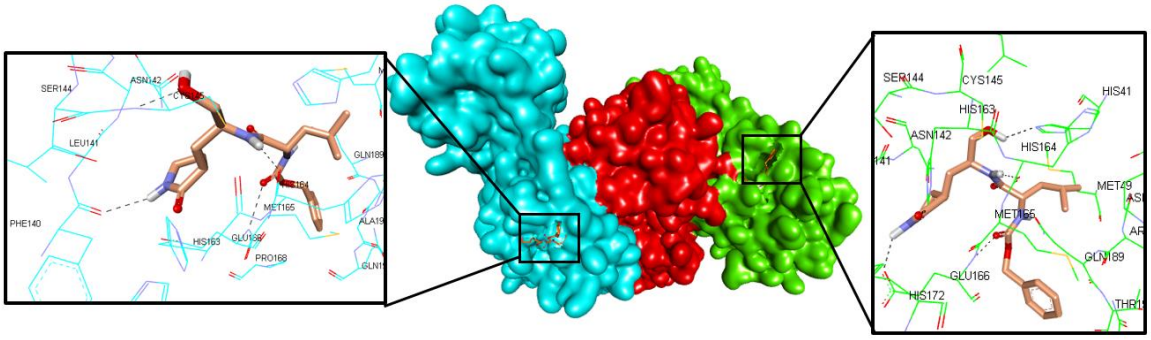

Figure 6. The trimer structure of 3CLpro as indicated by blue (monomer A), red (monomer B) and green (monomer C) surface model. Inset is the ligand complex to active site of the enzyme (presented by blue stick and green stick, for monomer A and monomer C, respectively). presented in a stick model (orange = C, white = H, blue = N and red = O). The H-bond is presented in black dot lines, respectively.

A class of imidazole-4-carboxamide compound was also complexed to SARS-Coronavirus-2 3CLpro and the 3D crystal structure was resolved at 1.46Å (PDB ID 6W79; Figure 7a) [103]. This inhibitor binds to the active site of the protease by interacting with the residues GLY143 and GLU166 at atom O (C=O-amide) and also the next O (C=O-amide), respectively. The hydrophobic interaction was also performed via the interaction between ASN142- O (C=O-amide), THR26-H-CH-imidazole), CYS145-imidazole ring, LEU141-ASN142-pyridine.

An inhibitor which was a repurposed drug from antineoplastic, complexed with SARS-Coronavirus-2 3CLpro in 1.60Å of 3D-crystal resolution (PDB ID 7BUY; Figure 7b) [104]. Interestingly, this inhibitor binds covalently (distance 1.8Å) at its O (C=O) to CYS145 which is one of the catalytic situ residues. This inhibitor's name is carmofur bearing hexylcarbamide acid structure, in which the fatty acid tail occupies the hydrophobic S2 subsite. A study reported that carmofur inhibits viral replication in cells (EC_{50} = 24.30 μM) and is a promising lead compound to develop new antiviral treatment for SARS-Coronavirus-2.

A more diverse inhibitor's structure was observed from the 3D-crystal structure with PDB ID 5RGG which was resolved at 2.26Å of resolution [105]; Figure 7c). The inhibitor is a carboxamide derivative namely 4-methyl-*N*-phenylpiperazine-1-carboxamide, binds at HIS80 via H-bond interaction. Instead of H-bond, HIS80 was also interact with the inhibitor via hydrophobic interaction which was co-bound with LYS90. This experiment could give an insight understanding

that even small molecule is able to bind to the protease, however, the potency of such inhibitor could be low due to the larger cavities whic need an extending occupation.

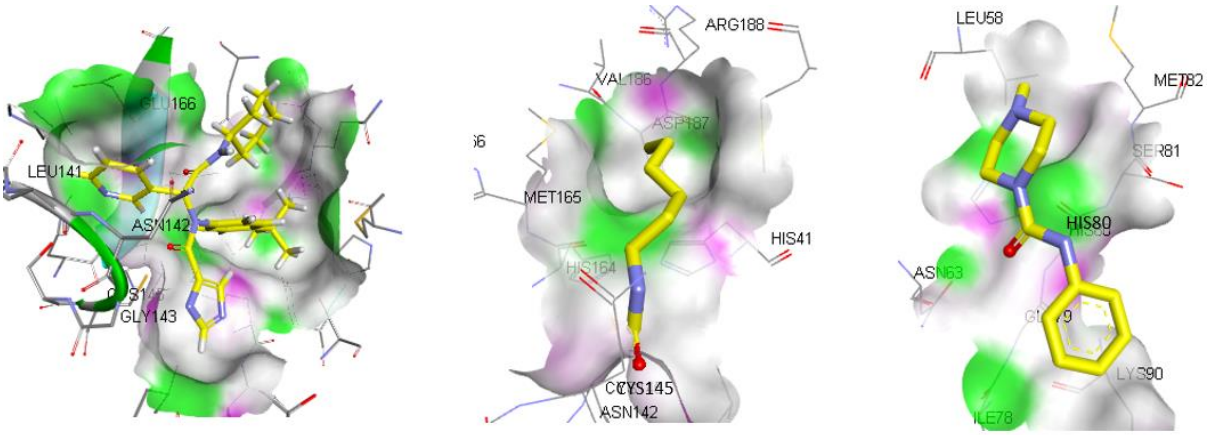

Figure 7. The presentation of a) imidazole-4-carboxamide, b) carmofur, and c) 4-methyl-N-phenylpiperazine-1-carboxamide bound into the active site of SARS-Coronavirus-2 3CLpro. The protein is visualized in surface model with the green area = hydrogen bond acceptor residues, white area = neutral residues, and magenta area = hydrogen bond donor residues. The ligands are presented in a stick form with yellow = C, white = H, blue = N, and red = O.

Table 2. The list of 3CLpro 3D-crystal structure available in protein data bank.

PDB ID	Co-crystallized Ligand	Resolution (Å)	Reference
6M2N	5,6,7-trihydroxy-2-phenyl-4H-chromen-4-one	2.20	[101]
6M2Q	-	1.70	[101]
6WQF	-	2.30	[106]
6XB1	1-ethyl-pyrrolidine-2,5-dione	1.80	[107]
6XB0	dimethyl sulfoxide	1.80	[107]
6XB2	1-ethyl-pyrrolidine-2,5-dione, dimethyl sulfoxide	2.10	[107]
6L00 and 6LNY	(2~{*S*})-4-methyl-~{*N*}-[(2~{*S*})-1-oxidanylidene-3-[(3~{*S*})-2-oxidanylidenepyrrolidin-3-yl]propan-2-yl]-2-[[(~{*E*})-3-phenylprop-2-enoyl]amino]pentanamide	1.94 and 2.25	[108]
7JFQ	1,2-ethanediol, formic acid	1.55	[109]
6XKF	1,2-ethanediol, chloride ion	1.80	[110]
6XKH	1,2-ethanediol, acetate ion, formic acid	1.28	[111]
6XOA	1,2-ethanediol	2.10	[112]
6LNQ	*N*-[(2*S*)-3-methyl-1-[[(2*S*)-4-methyl-1-oxidanylidene-1-[[(2*S*)-1-oxidanylidene-3-[(3*S*)-2-oxidanylidenepyrrolidin-3-yl]propan-2-yl]amino]pentan-2-yl]amino]-1-oxidanylidene-butan-2-yl]-1H-indole-2-carboxamide	2.24	[108]

7JUN	-	2.30	[113]
7JR3	-	1.55	[114]
7JR4	-	1.55	[115]
6XHU	-	1.80	[116]
6XQT	(1*R*,2*S*,5*S*)-3-[*N*-({1-[(*tert*-butylsulfonyl)methyl]cyclohexyl}carbamoyl)-3-methyl-*L*-valyl]-*N*-{(1*S*)-1-[(1*R*)-2-(cyclopropyla mino)-1-hydroxy-2-oxoethyl]pentyl}-6,6-dimethyl-3-azabicyclo[3.1.0]hexane-2-carboxamide	2.30	[117]
6XQS	(1*S*,3a*R*,6a*S*)-2-[(2*S*)-2-({(2*S*)-2-cyclohexyl-2-[(pyrazin-2-ylcarbonyl)amino]acetyl}amino)-3,3-dimethylbutanoyl]-*N*-[(2*R*,3*S*)-1-(cyclopropylamino)-2-hydroxy-1-oxohexan-3-yl]octahydrocyclopenta[c]pyrrole-1-carboxamide	1.90	[117]
6XQU	boceprevir (bound form)	2.20	[117]
6W2A	[4,4-*bis*(fluoranyl)cyclohexyl]methyl ~{*N*}-[(2~{*S*})-1-[[(1~{*R*},2~{*S*})-1-[*bis*(oxidanyl)-oxidanylidene-$l^{5}-sulfanyl]-1-oxidanyl-3-[(3~{*S*})-2-oxidanylidenepyrrolidin-3-yl]propan-2-yl]amino]-4-methyl-1-oxidanylidene-pentan-2-yl]carbamate, (1*S*,2*S*)-2-[(*N*-{[(4,4-difluorocyclohexyl)methoxy]carbonyl}-*L*-leucyl)amino]-1-hydroxy-3-[(3*S*)-2-oxopyrrolidin-3-yl]propane-1-sulfonic acid	1.65	[118]
6WTK	*N*~2~-[(benzyloxy)carbonyl]-*N*-{(2*S*)-1-hydroxy-3-[(3*S*)-2-oxopyrrolidin-3-yl]propan-2-yl}-*L*-leucinamide	2.00	[119]
6WTM	-	1.85	[119]
6WTJ	(1*S*,2*S*)-2-({*N*-[(benzyloxy)carbonyl]-*L*-leucyl}amino)-1-hydroxy-3-[(3*S*)-2-oxopyrrolidin-3-yl]propane-1-sulfonic acid	1.90	[119]
6W63 and 6W79	*N*-(4-tert-butylphenyl)-*N*-[(1R)-2-(cyclohexylamino)-2-oxo-1-(pyridin-3-yl)ethyl]-1H-imidazole-4-carboxamide	2.10	[103]
6WCO	N-(4-tert-butylphenyl)-N-[(1R)-2-(cyclopentylamino)-2-oxo-1-(pyridin-3-yl)ethyl]-1H-imidazole-4-carboxamide	1.48	[103]
6XBH	-	1.60	[120]
6XBG	-	1.45	[121]
6XFN	-	1.70	[122]
7JU7	Masitinib	1.60	[123]
3SZN	ethyl (4*R*)-4-({*N*-[(benzyloxy)carbonyl]-l-phenylalanyl}amino)-5-[(3*S*)-2-oxopyrrolidin-3-yl]pentanoate	1.69	[124]
3SNE	2-(*N*-morpholino)-ethanesulfonic acid	2.60	[125]
3SNA, 3SNB, and 3SNC	-	3.05, 2.40 and 2.58	[125]
6XBI	-	1.70	[126]
6XHO	ethyl (2*E*,4*S*)-4-{[*N*-(4-methoxy-1H-indole-2-carbonyl)-*L*-leucyl]amino}-5-[(3S)-2-oxopyrrolidin-3-yl]pent-2-enoate	1.45	[127]
6XHN	(3S)-3-{[*N*-(4-methoxy-1H-indole-2-carbonyl)-*L*-leucyl]amino}-2-oxo-4-[(3*S*)-2-oxopyrrolidin-3-yl]butyl 2-cyanobenzoate	1.38	[127]
6XHL and 6XHM	*N*-[(2*S*)-1-({(2*S*)-4-hydroxy-3-oxo-1-[(3*S*)-2-oxopyrrolidin-3-yl]butan-2-yl}amino)-4-methyl-1-oxopentan-2-yl]-4-methoxy-1H-indole-2-carboxamide	1.47 and 1.41	[127]
6XA4	-	1.65	[128]
6Y2E	-	1.75	[129]
6Y2G, 6Y2F	~{*tert*}-butyl~{*N*}-[1-[(2~{*S*})-3-cyclopropyl-1-oxidanylidene-1-[[(2~{*S*},3~{*R*})-3-oxidanyl-4-oxidanylidene-1-[(3~{*S*})-2-oxidanylidenepyrrolidin-3-yl]-4-	2.20, and 1.95	[129]

	[(phenylmethyl)amino]butan-2-yl]amino]propan-2-yl]-2-oxidanylidene-pyridin-3-yl]carbamate		
7JKV	*N*-[(2*S*)-1-({(1*S*,2*S*)-1-(1,3-benzothiazol-2-yl)-1-hydroxy-3-[(3S)-2-oxopyrrolidin-3-yl]propan-2-yl}amino)-4-methyl-1-oxopentan-2-yl]-4-methoxy-1H-indole-2-carboxamide	1.25	[130]
5RHF	1-acetyl-*N*-methyl-*N*-phenylpiperidine-4-carboxamide	1.76	[105]
5RHE	1-acetyl-*N*-(6-methoxypyridin-3-yl)piperidine-4-carboxamide	1.56	[105]
5RGG	4-methyl-*N*-phenylpiperazine-1-carboxamide	2.26	[105]
5RG1	*N*-alpha-acetyl-*N*-(3-bromoprop-2-yn-1-yl)-*L*-tyrosinamide	1.57	[105]
5RGH	5-fluoro-1-[(5-methyl-1,3,4-thiadiazol-2-yl)methyl]-1,2,3,6-tetrahydropyridine	1.70	[105]
5RGR	*N*,1-dimethyl-N-(propan-2-yl)-1H-pyrazolo[3,4-d]pyrimidin-4-amine	1.41	[105]
5RG3	*N*~2~-acetyl-*N*~1~-prop-2-en-1-yl-*L*-aspartamide	1.58	[105]
5RG2	*N*~2~-acetyl-*N*-prop-2-en-1-yl-*D*-allothreoninamide	1.63	[105]
5RGS	[(2~{*R*})-4-(phenylmethyl)morpholin-2-yl]methanol	1.72	[105]
5RGK	2-fluoro-*N*-[2-(pyridin-4-yl)ethyl]benzamide	1.43	[105]
5RGJ	(5*S*)-7-(pyrazin-2-yl)-2-oxa-7-azaspiro[4.4]nonane	1.34	[105]
5RGM	*N*'-acetyl-4,5,6,7-tetrahydro-1-benzothiophene-2-carbohydrazide	2.04	[105]
5RGM	*N*'-acetyl-4,5,6,7-tetrahydro-1-benzothiophene-2-carbohydrazide	2.04	[105]
5RG0	1,1'-(piperazine-1,4-diyl)di(ethan-1-one)	1.72	[105]
5RGN	1-{4-[(4-methylphenyl)sulfonyl]piperazin-1-yl}ethan-1-one	1.86	[105]
5RGQ	1-(4-fluoro-2-methylphenyl)methanesulfonamide	2.15	[105]
5RGP	1-{4-[(2,4-dimethylphenyl)sulfonyl]piperazin-1-yl}ethan-1-one	2.07	[105]
5R8T	-	1.27	[105]
5RGZ	2-(3-cyanophenyl)-*N*-(pyridin-3-yl)acetamide	1.52	[105]
5RHA	1-{4-[(thiophen-2-yl)methyl]piperazin-1-yl}ethan-1-one	1.51	[105]
5RH3	(2*R*)-2-(3-chlorophenyl)-*N*-(4-methylpyridin-3-yl)propanamide	1.69	[105]
5RH4	(2*R*)-2-(6-chloro-9H-carbazol-2-yl)propanoic acid	1.34	[105]
5RGU	*N*-(3-{[(2*R*)-4-oxoazetidin-2-yl]oxy}phenyl)-2-(pyrimidin-5-yl)acetamide	2.11	[105]
5RH6	*N*-[(1*R*)-2-[(2-ethyl-6-methylphenyl)amino]-2-oxo-1-(pyridin-3-yl)ethyl]-*N*-[6-(propan-2-yl)pyridin-3-yl]propanamide	1.60	[105]
5RGT	*N*-[(1*R*)-2-(tert-butylamino)-2-oxo-1-(pyridin-3-yl)ethyl]-*N*-(5-tert-butyl-1,2-oxazol-3-yl)propanamide	2.22	[105]
5RH5	*N*-(5-tert-butyl-1,2-oxazol-3-yl)-*N*-[(1*R*)-2-[(4-methoxy-2-methylphenyl)amino]-2-oxo-1-(pyridin-3-yl)ethyl]propanamide	1.72	[105]
5RGW	2-(5-cyanopyridin-3-yl)-N-(pyridin-3-yl)acetamide	1.43	[105]
5RH8	2-(cyanomethoxy)-*N*-[(1,2-thiazol-4-yl)methyl]benzamide	1.81	[105]
5RGV	2-(isoquinolin-4-yl)-*N*-phenylacetamide	1.82	[105]
5RH7	*N*-(5-tert-butyl-1H-pyrazol-3-yl)-*N*-[(1R)-2-[(2-ethyl-6-methylphenyl)amino]-2-oxo-1-(pyridin-3-yl)ethyl]propanamide	1.71	[105]
5RGY	*N*-(4-methoxypyridin-2-yl)-2-(naphthalen-2-yl)acetamide	1.976	[105]
5RGX	2-(3-cyanophenyl)-*N*-(4-methylpyridin-3-yl)acetamide	1.69	[105]
5RH9	*N*-{4-[(1*S*)-1-methoxyethyl]phenyl}-*N*-[(1*R*)-2-[(4-methoxy-2-methylphenyl)amino]-2-oxo-1-(pyridin-3-yl)ethyl]propanamide	1.91	[105]
5RH0	*N*-(5-methylthiophen-2-yl)-*N*'-pyridin-3-ylurea	1.92	[105]
5RH2	2-(3-chlorophenyl)-*N*-(4-methylpyridin-3-yl)acetamide	1.83	[105]
5RH1	2-(5-chlorothiophen-2-yl)-*N*-(pyridin-3-yl)acetamide	1.96	[105]
5REA	(azepan-1-yl)(2H-1,3-benzodioxol-5-yl)methanone	1.63	[105]
5REB	1-[(thiophen-3-yl)methyl]piperidin-4-ol	1.68	[105]
5REC	2-{[(1H-benzimidazol-2-yl)amino]methyl}phenol	1.73	[105]

5REE	(2*R*,3*R*)-1-benzyl-2-methylpiperidin-3-ol	1.77	[105]
7JVZ	-	2.50	[131]
6W9Q	-	2.05	[132]
7BRR	(1*S*,2*S*)-2-({*N*-[(benzyloxy)carbonyl]-L-leucyl}amino)-1-hydroxy-3-[(3*S*)-2-oxopyrrolidin-3-yl]propane-1-sulfonic acid	1.40	[133]
7BRO	-	2.00	[134]
7BRP	(1*R*,2*S*,5*S*)-*n*-[(1*S*)-3-amino-1-(cyclobutylmethyl)-2,3-dioxopropyl]-3-[(2*S*)-2-{[(tert-butylamino)carbonyl]amino}-3,3-dimet hylbutanoyl]-6,6-dimethyl-3-azabicyclo[3.1.0]hexane-2-carboxamide	1.80	[135]
7C2Q	-	1.93	[136]
7C8T	*N*-[(benzyloxy)carbonyl]-*O*-(*tert*-butyl)-l-threonyl-3-cyclohexyl-*N*-[(1*S*)-2-hydroxy-1-{[(3*S*)-2-oxopyrrolidin-3-yl]methyl}ethyl]-l-alaninamide	2.05	[137]
7C8R	Ethyl (4*R*)-4-[[(2*S*)-4-methyl-2-[[(2*S*,3*R*)-3-[(2-methylpropan-2-yl)oxy]-2-(phenylmethoxycarbonylamino)butanoyl]amino]pentanoyl]amino]-5-[(3*S*)-2-oxidanylidenepyrrolidin-3-yl]pentanoate	2.30	[137]
6XCH	-	2.20	[138]
6L70	(1*S*,2*S*)-2-({*N*-[(benzyloxy)carbonyl]-L-leucyl}amino)-1-hydroxy-3-[(3*S*)-2-oxopyrrolidin-3-yl]propane-1-sulfonic acid	1.56	[139]
6FV1	(2~{*S*})-4-methyl-~{*N*}-[(2~{*S*},3~{*R*})-3-oxidanyl-4-oxidanylidene-1-[(3~{*S*})-2-oxidanylidenepyrrolidin-3-yl]-4-[(phenylmethyl)amino]butan-2-yl]-2-[[(~{*E*})-3-phenylprop-2-enoyl]amino]pentanamide	2.30	[140]
6FV2	(*S*)-*N*-benzyl-3-((*S*)-2-cinnamamido-3-phenylpropanamido)-2-oxo-4-((*S*)-2-oxopyrrolidin-3-yl)butanamide	2.95	[140]
7D31	(3~{*S*},3~{a}~{*S*},6~{a}~{*R*})-2-[3-[3,5-bis(fluoranyl)phenyl]propanoyl]-~{*N*}-[(2~{*S*})-1-oxidanylidene-3-[(3~{*S*})-2-oxidanylidenepyrrolidin-3-yl]propan-2-yl]-3,3~{a},4,5,6,6~{a}-hexahydro-1~{H}-cyclopenta[c]pyrrole-3-carboxamide 2	2.00	[141]
7D1O	(1*R*,2*S*,5*S*)-3-[*N*-({1-[(*tert*-butylsulfonyl)methyl]cyclohexyl}carbamoyl)-3-methyl-*L*-valyl]-*N*-{(1*S*)-1-[(1*R*)-2-(cyclopropyla mino)-1-hydroxy-2-oxoethyl]pentyl}-6,6-dimethyl-3-azabicyclo[3.1.0]hexane-2-carboxamide	1.78	[142]
7C7P	(1*S*,3a*R*,6a*S*)-2-[(2*S*)-2-({(2*S*)-2-cyclohexyl-2-[(pyrazin-2-ylcarbonyl)amino]acetyl}amino)-3,3-dimethylbutanoyl]-*N*-[(2*R*,3*S*)-1-(cyclopropylamino)-2-hydroxy-1-oxohexan-3-yl]octahydrocyclopenta[c]pyrrole-1-carboxamide (3~{*S*},3~{a}~{*S*},6~{a}~{*R*})-~{*N*}-[(2~{*R*},3~{S})-1-(cyclopropylamino)-2-oxidanyl-1-oxidanylidene-hexan-3-yl]-2-methanoyl-3,3~{a},4,5,6,6~{a}-hexahydro-1~{H}-cyclopenta[c]pyrrole-3-carboxamide	1.74	[143]
7COM	boceprevir (bound form)	2.25	[144]
6ZRU	boceprevir (bound form)	2.10	[145]
6ZRT	(1*S*,3a*R*,6a*S*)-2-[(2*S*)-2-({(2*S*)-2-cyclohexyl-2-[(pyrazin-2-ylcarbonyl)amino]acetyl}amino)-3,3-dimethylbutanoyl]-*N*-[(2*R*,3*S*)-1-(cyclopropylamino)-2-hydroxy-1-oxohexan-3-yl]octahydrocyclopenta[c]pyrrole-1-carboxamide	2.10	[146]
6MOK	-	5.10	[147]

6LZE	~{*N*}-[(2~{*S*})-3-cyclohexyl-1-oxidanylidene-1-[[(2~{*S*})-1-oxidanylidene-3-[(3~{*S*})-2-oxidanylidenepyrrolidin-3-yl]propan-2-yl]amino]propan-2-yl]-1~{H}-indole-2-carboxamide	1.50	[148]
7C6S	boceprevir (bound form)	1.60	[149]
7CX9	3-iodanyl-1~{H}-indazole-7-carbaldehyde	1.73	[150]

5. Biflavonoid as The Protease –Inhibitor

Although it is not so many, there is a few study of biflavonoid-class compounds reporting their activities as protease inhibitors. Amentoflavone from *Torreya nucifera* was the early biflavonoid studied its inhibitory activity against SARS-CoV 3CLpro by showing IC_{50} 8.3 µM. The results were compared to three types of flavonoid (apigenin, luteolin and quercetin) which showed less inhibition and therefore, the structure-activity relationships were generated to confirm that the more potent activity of biflavonoid appeared to be associated with the presence of benzene ring moiety at position C-3' of flavones, as biflavone had an effect on 3CLpro inhibitory activity [36]. Based on the Ryu et al. finding, a QSAR study of biflavonoid and its analogs were carried out to generate a QSAR model defining that increasing value of the dipole moment along X-axis may be conducive to the activity. Therefore, the steric character of this part may be favorable for its activity. Compounds having higher dipole moment due to the much bulky aryl groups, therefore, have a higher activity than the compound having less bulky aryl group [23].

The antiproteolytic activity of biflavonoid was early determined on morelloflavone-4'''-*O*-*β*-*D*-glycosyl, (±)-fukugiside, and morelloflavone. These biflavonoids were isolated from the fruit epocarp of *Garcinia brasiliensis* which further semisynthesized into three moreflavone derivatives i.e. morelloflavone-7,4',7'',3''',4''''- penta-*O*-acetyl, morelloflavone-7,4',7'',3''',4'''-penta-*O*-methyl and morelloflavone-7,4',7'',3''',4'''-penta-*ſ*-butanoyl. A high inhibitory activity was demonstrated by these biflavonioid against r-CPB2.8 and r-CPB3 isoforms which are papain-like protease of *Leismania mexicana* with IC_{50} 0.42-1.01 µM for four the most active compounds. Interestingly, there was no cytotoxic activity towards normal cell lines as observed from the *in vitro* study [151].

Further study was pursued by the same research group in evaluating those biflavonoid activities against the cysteine protease (papain and cruzain) and serine protease of *Trypanozoma cruzii*. All biflavonoid compounds demonstrated excellent inhibitions toward all protease enzymes (IC_{50} 0.02-106 µM), however, morelloflavone-7,4',7'',3''',4''''- penta-O-acetyl showed the best activity which might be due to the carbonyl group in the structure. This functional group could

favor a higher nucleophilic attack by serine and cysteine proteases. This agreed with morelloflavone-7,4',7'',3''',4'''-penta-*O*-methyl (IC_{50} = 15.4 ± 0.7 µM for papain), in which the compound having no carbonyl group in structure, was less active in the inhibition process. This was confirmed by the structure–activity relationships (SARs) study had been performed using flexible docking simulations [152].

A study by Assis et al. reported fukugetin, a biflavone originated from *Garcinia brasiliensis*, demonstrated partital competitive and hyperbolic-mix type inhibitions against the major cystein protease of *Trypanosoma cruzii* (cruzain and papain), respectively. The potency of such biflavone was expressed in a slow reversible type inhibition with K_i 1.1 and 13.4 µM for cruzain and papain, respectively, describing that the biflavone has 12 time faster inhibition toward cruzain than papain in inhibiting the enzymes. The molecular docking study predicted that this activity is due to the chemical interaction between biflavone at ring C with S3 pocket, whereas the ring C' binds at S2 pocket through hydrogen bond as well as hydrophobic interactions [153].

A virtual screening was performed to identify the hits of tryptase inhibitor followed by in vitro experiments to identify the lead compounds. Tryptase is a class of serine protease enzyme released as the allergic response such as skin inflammation and asthma, from the mast cells. Off to 98,000 compounds screened, 2.28% of the library (2503 compouns) were selected as the hits. Interestingly, biflavonoids were one of the most frequently represented in the 200 compounds with the strongest tryptase binding energy. Using FRET-based assay, these 200 compounds were further in vitro sreened to afford the lead compound, and then biflavonoid podocorpus flavone A blocks tryptase activity by 61.6.%. The docking study suggested that the biflavonoid is favorably binding at the S4 of tryptase [154].

Biflavonoid was also reported to down regulate the expression of matrix metalloproteinase-1 (MMP-1) from human skin fibroblast. MMP is a zymogen (zinc-dependent peptidase) which degrades the extracellular matrix to perform angiogenesis, inflammation, cell migration and tissue remodelling. The high expression of this enzyme is often associated with cancer and wound diabetic foot ulcer. 2',8''-biapigenin, sumaflavone, taiwaniaflavone, amentoflavone, and robustaflavone were isolated from *Selaginella tamariscina* showed significant MMP-1 inhibitory activity in primary human dermal fibroblasts after UV irradiation. The IC_{50} values of sumaflavone, amentoflavone and retinoic acid (used as the positive control) were 0.78, 1.8, and 10 µM, respectively [155].

6. Perspectives

Two main protein targets in coronaviral genome are classified into structural and non-structural protein. Structural protein which is composed by membrane, envelope, and nucleocapsid are formed in the inner viral cell, whereas the spike protein is located in the outer cell [156, 157]. It might be difficult to control the activity of such structural protein because they roles the virus' life during the viral cell assembly which could be too fast too control. Most likely, the host will be suddenly infected by the virus while there is no time to block the activity of S protein during viral-host attachment as well as its endocytosis. Therefore, designing the protein inhibitor for coronavirus, the non-structural protein could be more favorable than the structural protein due to its role in controlling the polypeptide proteolytic, reverse transcription, RNA replication as well as the protein translation, which might take more time than the viral assembly.

Among the 16 nonstructural proteins, NSP5 are the most attractive targets while others are still elusive [158]. The NSP5 main protease (3CLpro) is the most common targeted protein in coronavirus because they are formed in the host and acting during cleavage and post-translational polyprotein synthesis, thus it is relatively easier to control their activities. Two classes of compound are reported having these protein activities, including peptide and nonpeptide compound. Naturally, the protease has peptide substrate due to its function to hydrolyse the peptide bond upon proteolysis. Therefore, for competitive inhibitor, compound having peptide-like structure should be suitable to block the enzyme-substrate binding. There are notable peptide (like) compounds demonstrating low micromolar activity towards the protease such as lopinavir and ritonavir [159]. Although peptide is the suitable structure designed for the protease inhibitor, however, the physic-chemical properties of this class of compound often make it fails under clinical trials. Peptide has a number of flexible bond which makes it energetically unstable either during preparation or its pharmacokinetic stage. The structure is mimicking protein, therefore it is sensitive towards denaturation and hydrolysis during preparation. At the pharmacokinetic stage especially during absorption, peptide is less absorbed due to its isoelectric character which makes it very polar in aqueous bilological fluids thus is hard to penetrate the intestinal membrane lipid bilayer [160]. This causes the peptide becomes unsuitable for oral preparation which needs absorption process. Other alternative is formulated in parentral preparation, however, this is costly and not applicable administered by patient themselves. Therefore, peptide is practically used as

the model only and then should be further modified to more rigid character to improve the stability. One effort has been conducted to formulate the drug delivery system to improve the bioavailability such as using liposome technology, however, the use of organic solvents in the liposome dosage form could make it toxic [161, 162].

Non-peptide or often called as small molecule inhibitors, currently takes more attention used as the molecule target for protease inhibitors. The presence of aromatic rings could make the compound is energetically more stable than the peptide due to its rigid character [163]. The rigid character makes the entropy of the compound to be less thus stabilizing the compound-enzyme affinity upon binding. The non-peptide inhibitor is still can be divided into natural and synthetic compound. Natural compound is unique structure due to the presence of chiral carbon which could make the ligand-protein binding become more specific. A class of biflavonoid showed *in vitro* competitive inhibition in low micromolar activities towards the protease which agreed with the docking explanation. Amentoflavone is the early biflavonoid found active against 3CLpro of SARS-Coronavirus underlining the potency of such compound to be this protease inhibitor. It was postulated that the presence of benzene ring moiety at position C-3' of flavones, as biflavone had an effect on 3CLpro inhibitory activity. The synthetic (semi synthetic) biflavonoids are the further strategy to get the product being more feasible to be developed as protease inhibitor. Compounds bearing more carbonyl groups seems like promising as this protease inhibitor as it is designed to favor a higher nucleophilic attack by serine and cysteine proteases, using molecular docking.

3CLpro is still the most recommended protein target in the discovery of anti-SARS coronaviral agent. The availability of crystal structure sand its high conserve binding site, makes the structure based drug design becomes applicable [164, 165]. The structure-based drug design is also able to combine with ligand-based drug design since the structure information of the compounds either in peptide or non-peptide, have been reported as the protease inhibitors. The non-peptide compound such as biflavonoid provide more promising candidate to enter either pre- or clinical stage due to its more stable physic-chemical properties during preparation as well as pharmacokinetics.

7. Conclusion

In conclusion, our review strongly recommend that biflavonoid, either from natural product or its synthetic is very potential to be used as of SARS-Coronavirus-2 3CLpro inhibitor. Its dimer and big structure are more suitable for 3CLpro binding site composing two beta barrels than the

corresponding flavones. To the best of our knowledge, this is the first review to describe the potential inhibitory effects of biflavonoid against 3CLpro. Thus, we believe that this compound may be a good candidate for development as a natural therapeutic drug against SARS-Coronavirus-2 infection.

Reference

[1] Djalante, R., Lassa, J., Setiamarga, D., Mahfud, C., Sudjatma, A., Indrawan, M., ... & Gunawan, L. A. (2020). Review and analysis of current responses to COVID-19 in Indonesia: Period of January to March 2020. Progress in Disaster Science, 6, 100091. https://doi.org/10.1016/j.pdisas.2020.100091

[2] World Health Organization. WHO coronavirus disease (covid-19) dashboard, https://covid19.who.int/ ; 2020 (accessed 24 October 2020).

3. Kompas.com, Data covid-19 di Indonesia, https://www.kompas.com/covid-19; 2020 (accessed 24 October 2020).

4. United Nations Industrial Development Organization, Corionavirus, the economic impact-10 July 2020, https://www.unido.org/stories/coronavirus-economic-impact-10-july-2020; 2020 (accessed 24 October 2020).

5. Dhama, K., Patel, S. K., Sharun, K., Pathak, M., Tiwari, R., Yatoo, M. I., ... & Singh, K. P. (2020). SARS-CoV-2 jumping the species barrier: zoonotic lessons from SARS, MERS and recent advances to combat this pandemic virus. Travel medicine and infectious disease, 37, 101830.

6. Hosseini, E. S., Kashani, N. R., Nikzad, H., Azadbakht, J., Bafrani, H. H., & Kashani, H. H. (2020). The novel coronavirus Disease-2019 (COVID-19): Mechanism of action, detection and recent therapeutic strategies. Virology, 551, 1-9.

7. Prasad, N., Gopalakrishnan, N., Sahay, M., Gupta, A., Agarwal, S. K., & behalf of COVID, O. (2020). Epidemiology, genomic structure, the molecular mechanism of injury, diagnosis and clinical manifestations of coronavirus infection: An overview. Indian Journal of Nephrology, 30(3), 143.

8. Snijder, E. J., Decroly, E., & Ziebuhr, J. (2016). The nonstructural proteins directing coronavirus RNA synthesis and processing. In Advances in virus research (Vol. 96, pp. 59-126). Academic Press.

9. Shereen, M. A., Khan, S., Kazmi, A., Bashir, N., & Siddique, R. (2020). COVID-19 infection: Origin, transmission, and characteristics of human coronaviruses. Journal of Advanced Research, 24, 91-98.

10. Grum-Tokars, V., Ratia, K., Begaye, A., Baker, S. C., & Mesecar, A. D. (2008). Evaluating the 3C-like protease activity of SARS-Coronavirus: recommendations for standardized assays for drug discovery. Virus research, 133(1), 63-73.

11. Joshi, S., Joshi, M., & Degani, M. S. (2020). Tackling SARS-CoV-2: proposed targets and repurposed drugs. Future medicinal chemistry, 12(7), 1579-1601. https://doi.org/10.4155/fmc-2020-0147

12. Báez-Santos, Y. M., John, S. E. S., & Mesecar, A. D. (2015). The SARS-coronavirus papain-like protease: structure, function and inhibition by designed antiviral compounds. Antiviral research, 115, 21-38.

13. Colunga Biancatelli, R. M. L., Berrill, M., Catravas, J. D., & Marik, P. E. (2020). Quercetin and vitamin C: an experimental, synergistic therapy for the prevention and treatment of SARS-CoV-2 related disease (COVID-19). Frontiers in immunology, 11, 1451.

14. Chojnacka, K., Witek-Krowiak, A., Skrzypczak, D., Mikula, K., & Młynarz, P. (2020). Phytochemicals containing biologically active polyphenols as an effective agent against Covid-19-inducing coronavirus. Journal of Functional Foods, 73, 104146. https://doi.org/10.1016/j.jff.2020.104146

15. Jain R, Shukla S, Nema N, Panday A, Gour HS (2020) A Systemic Review: Structural Mechanism of SARS-CoV-2A and promising

16. Preventive Cure by Phytochemicals. J AgriSci Food Res 11: 274. doi: 10.35248/2593-9173.20.11.274 Li, S. Y., Chen, C., Zhang, H. Q., Guo, H. Y., Wang, H., Wang, L., ... & Li, R. S. (2005). Identification of natural compounds with antiviral activities against SARS-associated coronavirus. Antiviral research, 67(1), 18-23.

17. Lin, C. W., Tsai, F. J., Tsai, C. H., Lai, C. C., Wan, L., Ho, T. Y., ... & Chao, P. D. L. (2005). Anti-SARS coronavirus 3C-like protease effects of Isatis indigotica root and plant-derived phenolic compounds. Antiviral research, 68(1), 36-42.

18. Schwarz, S., Sauter, D., Wang, K., Zhang, R., Sun, B., Karioti, A., ... & Schwarz, W. (2014). Kaempferol derivatives as antiviral drugs against the 3a channel protein of coronavirus. Planta medica, 80(02-03), 177.

19. Cinatl, J., Morgenstern, B., Bauer, G., Chandra, P., Rabenau, H., & Doerr, H. W. (2003). Glycyrrhizin, an active component of liquorice roots, and replication of SARS-associated coronavirus. The Lancet, 361(9374), 2045-2046.

20. Kim, D. E., Min, J. S., Jang, M. S., Lee, J. Y., Shin, Y. S., Park, C. M., ... & Kwon, S. (2019). Natural bis-benzylisoquinoline alkaloids-tetrandrine, fangchinoline, and cepharanthine, inhibit human coronavirus OC43 infection of MRC-5 human lung cells. Biomolecules, 9(11), 696.

21. Müller, C., Schulte, F. W., Lange-Grünweller, K., Obermann, W., Madhugiri, R., Pleschka, S., ... & Grünweller, A. (2018). Broad-spectrum antiviral activity of the eIF4A inhibitor silvestrol against corona-and picornaviruses. Antiviral research, 150, 123-129.

22. Jamiu, A. T., Aruwa, C. E., Abdulakeem, I. A., Ajao, A. A., & Sabiu, S. (2020). Phytotherapeutic Evidence Against Coronaviruses and Prospects for COVID-19. Pharmacognosy Journal, 12(6), 1252-1257. https://doi.org/10.5530/pj.2020.12.174

23. Adhikari, N., Baidya, S. K., Saha, A., & Jha, T. (2017). Structural Insight Into the Viral 3C-Like Protease Inhibitors: Comparative SAR/QSAR Approaches. In Viral Proteases and Their Inhibitors (pp. 317-409). Academic Press.

24. Di Cera, E. (2009). Serine proteases. IUBMB life, 61(5), 510-515.

25. Geiger, H., & Quinn, C. (1975). Biflavonoids. In The flavonoids (pp. 692-742). Springer, Boston, MA.

26. G Mercader, A., & B Pomilio, A. (2013). Naturally-occurring dimers of flavonoids as anticarcinogens. Anti-Cancer Agents in Medicinal Chemistry (Formerly Current Medicinal Chemistry-Anti-Cancer Agents), 13(8), 1217-1235.

27. Panche, A. N., Diwan, A. D., & Chandra, S. R. (2016). Flavonoids: an overview. Journal of nutritional science, 5, 1-15. https://doi.org/10.1017/jns.2016.41

28. Harborne, J. B., Marby, H., & Marby, T. J. (2013). The flavonoids. Springer.

29. Pietta, P. G. (2000). Flavonoids as antioxidants. Journal of natural products, 63(7), 1035-1042.

30. Cushnie, T. T., & Lamb, A. J. (2005). Antimicrobial activity of flavonoids. International journal of antimicrobial agents, 26(5), 343-356.

31. Mabry, T., Markham, K. R., & Thomas, M. B. (2012). The systematic identification of flavonoids. Springer Science & Business Media.

32. Oliveira, R. N., Mancini, M. C., Oliveira, F. C. S. D., Passos, T. M., Quilty, B., Thiré, R. M. D. S. M., & McGuinness, G. B. (2016). FTIR analysis and quantification of phenols and flavonoids of five commercially available plants extracts used in wound healing. Matéria (Rio de Janeiro), 21(3), 767-779.

33. March, R., & Brodbelt, J. (2008). Analysis of flavonoids: tandem mass spectrometry, computational methods, and NMR. Journal of mass spectrometry, 43(12), 1581-1617.

34. Okigawa, M.; Kawano, N. Tetrahed. Lett. 1973, 22, 2003.

35. Son, K. H.; Park, J. O.; Chung, K. C.; Chang, H. W.; Kim, H. P.; Kim, J. S.; Kang, S. S. Arch. Pharm. Res. 1992, 15, 365.

36. Ryu, Y. B., Jeong, H. J., Kim, J. H., Kim, Y. M., Park, J. Y., Kim, D., ... & Rho, M. C. (2010). Biflavonoids from Torreya nucifera displaying SARS-CoV 3CLpro inhibition. Bioorganic & medicinal chemistry, 18(22), 7940-7947.

37. Yu, S., Yan, H., Zhang, L., Shan, M., Chen, P., Ding, A., & Li, S. F. Y. (2017). A review on the phytochemistry, pharmacology, and pharmacokinetics of amentoflavone, a naturally-occurring biflavonoid. Molecules, 22(2), 299.

38. Feuereisen, M. M., Barraza, M. G., Zimmermann, B. F., Schieber, A., & Schulze-Kaysers, N. (2017). Pressurized liquid extraction of anthocyanins and biflavonoids from Schinus terebinthifolius Raddi: A multivariate optimization. Food chemistry, 214, 564-571.

39. Waterman, M. J., Nugraha, A. S., Hendra, R., Ball, G. E., Robinson, S. A., & Keller, P. A. (2017). Antarctic moss biflavonoids show high antioxidant and ultraviolet-screening activity. Journal of natural products, 80(8), 2224-2231.

40. Li, D., Qian, Y., Tian, Y. J., Yuan, S. M., Wei, W., & Wang, G. (2017). Optimization of ionic liquid-assisted extraction of biflavonoids from Selaginella doederleinii and evaluation of its antioxidant and antitumor activity. Molecules, 22(4), 586.

41. Chatsumpun, N., Sritularak, B., & Likhitwitayawuid, K. (2017). New biflavonoids with α-glucosidase and pancreatic lipase inhibitory activities from Boesenbergia rotunda. Molecules, 22(11), 1862.

42. Tabares-Guevara, J. H., Lara-Guzmán, O. J., Londoño-Londoño, J. A., Sierra, J. A., León-Varela, Y. M., Álvarez-Quintero, R. M., ... & Ramirez-Pineda, J. R. (2017). Natural Biflavonoids Modulate Macrophage–Oxidized LDL Interaction In Vitro and Promote Atheroprotection In Vivo. Frontiers in immunology, 8, 923.

43. Li, P., Yue, G. G. L., Kwok, H. F., Long, C. L., Lau, C. B. S., & Kennelly, E. J. (2017). Using ultra-performance liquid chromatography quadrupole time of flight mass spectrometry-based chemometrics for the identification of anti-angiogenic biflavonoids from edible Garcinia species. Journal of agricultural and food chemistry, 65(38), 8348-8355.

44. Gürbüz, P., & Doğan, Ş. D. (2017). Biflavonoids from Fumana procumbens (Dunal) Gren. & Godr. Biochemical Systematics and Ecology, 74, 57-59.

45. Recalde-Gil, M. A., Klein-Júnior, L. C., dos Santos Passos, C., Salton, J., de Loreto Bordignon, S. A., Monace, F. D., ... & Henriques, A. T. (2017). Monoamine oxidase inhibitory activity of biflavonoids from branches of Garcinia gardneriana (Clusiaceae). Natural Product Communications, 12(4), 1934578X1701200411.

46. Adem, F. A., Mbaveng, A. T., Kuete, V., Heydenreich, M., Ndakala, A., Irungu, B., ... & Efferth, T. (2019). Cytotoxicity of isoflavones and biflavonoids from Ormocarpum kirkii towards multi-factorial drug resistant cancer. Phytomedicine, 58, 152853.

47. Li, M., Li, B., Xia, Z. M., Tian, Y., Zhang, D., Rui, W. J., ... & Xiao, F. J. (2019). Anticancer effects of five biflavonoids from Ginkgo Biloba L. male flowers in vitro. Molecules, 24(8), 1496.

48. Yun-Ying, L. I., Xiao-Yan, L. U., Jia-Li, S. U. N., Qing-Qing, W. A. N. G., Zhang, Y. D., Zhang, J. B., & Xiao-Hui, F. A. N. (2019). Potential hepatic and renal toxicity induced by the biflavonoids from Ginkgo biloba. Chinese journal of natural medicines, 17(9), 672-681.

49. Linden, M., Brinckmann, C., Feuereisen, M. M., & Schieber, A. (2020). Effects of structural differences on the antibacterial activity of biflavonoids from fruits of the Brazilian peppertree (Schinus terebinthifolius Raddi). Food Research International, 109134.

50. Xu, J., Yang, L., Wang, R., Zeng, K., Fan, B., & Zhao, Z. (2019). The biflavonoids as protein tyrosine phosphatase 1B inhibitors from Selaginella uncinata and their antihyperglycemic action. Fitoterapia, 137, 104255.

51. Mendiratta, A., Dayal, R., Bartley, J. P., & Smith, G. (2017). A Phenylpropanoid and Biflavonoids from the Needles of Cephalotaxus harringtonia var. harringtonia. Natural Product Communications, 12(11), 1934578X1701201132.

52. Oliveira, P. D. A., Fidelis, Q. C., Fernandes, T. F. D. C., Souza, M. C. D., Coutinho, D. M., Prudêncio, E. R., ... & Marinho, B. G. (2019). Evaluation In Vivo and In Vitro of the

Antioxidant, Antinociceptive, and Anti-Inflammatory Activities of Biflavonoids From Ouratea hexasperma and O. ferruginea. Natural Product Communications, 14(6), 1934578X19856802.

53. Sirimangkalakitti, N., Juliawaty, L. D., Hakim, E. H., Waliana, I., Saito, N., Koyama, K., & Kinoshita, K. (2019). Naturally occurring biflavonoids with amyloid β aggregation inhibitory activity for development of anti-Alzheimer agents. Bioorganic & medicinal chemistry letters, 29(15), 1994-1997.

54. Yan, H. W., Zhu, H., Yuan, X., Yang, Y. N., Feng, Z. M., Jiang, J. S., & Zhang, P. C. (2019). Eight new biflavonoids with lavandulyl units from the roots of Sophora flavescens and their inhibitory effect on PTP1B. Bioorganic Chemistry, 86, 679-685.

55. Dziwornu, G. A., Toorabally, N. R., Bhowon, M. G., Jhaumeer-Laulloo, S., Sunassee, S., Moser, A., & Argyropoulos, D. (2017). Computer Assisted Structure Elucidation of Two Biflavonoids from the Leaves of Ochna Mauritiana. Planta Medica International Open, 4(S 01), Mo-PO.

56. Abdullah, I., Phongpaichit, S., Voravuthikunchai, S. P., & Mahabusarakam, W. (2018). Prenylated biflavonoids from the green branches of Garcinia dulcis. Phytochemistry Letters, 23, 176-179.

57. Ren, D., Meng, F. C., Liu, H., Xiao, T., Lu, J. J., Lin, L. G., ... & Zhang, Q. W. (2018). Novel biflavonoids from Cephalotaxus oliveri Mast. Phytochemistry Letters, 24, 150-153.

58. Zhang, X., Gao, R., Liu, Y., Cong, Y., Zhang, D., Zhang, Y., ... & Lu, C. (2019). Anti-virulence activities of biflavonoids from Mesua ferrea L. flower. Drug discoveries & therapeutics, 13(4), 222-227.

59. Carrillo-Hormaza, L., Ramírez, A. M., Quintero-Ortiz, C., Cossio, M., Medina, S., Ferreres, F., ... & Osorio, E. (2016). Comprehensive characterization and antioxidant activities of the main biflavonoids of Garcinia madruno: A novel tropical species for developing functional products. Journal of functional foods, 27, 503-516.

60. Jin, H., Cui, H., Yang, X., Xu, L., Li, X., Liu, R., ... & Song, X. (2018). Nematicidal activity against Aphelenchoides besseyi and Ditylenchus destructor of three biflavonoids, isolated from roots of Stellera chamaejasme. Journal of Asia-Pacific Entomology, 21(4), 1473-1478.

61. Xiao, S., Mu, Z. Q., Cheng, C. R., & Ding, J. (2019). Three new biflavonoids from the branches and leaves of Cephalotaxus oliveri and their antioxidant activity. Natural product research, 33(3), 321-327.

62. Zar Wynn Myint, K., Kido, T., Kusakari, K., Prasad Devkota, H., Kawahara, T., & Watanabe, T. (2019). Rhusflavanone and mesuaferrone B: tyrosinase and elastase inhibitory biflavonoids extracted from the stamens of Mesua ferrea L. Natural Product Research, 1-5. https://doi.org/10.1080/14786419.2019.1613395

63. Sun, Y., Shi, B., Gao, M., Fu, L., Chen, H., Hao, Z., ... & Feng, W. (2018). Two New Biflavonoids from the Roots and Rhizomes of Sinopodophyllum emodi. Chemistry of Natural Compounds, 54(4), 649-653.

64. Liu, Y., Kelsang, N., Lu, J., Zhang, Y., Liang, H., Tu, P., ... & Zhang, Q. (2019). Oxytrodiflavanone A and Oxytrochalcoflavanones A, B: New Biflavonoids from Oxytropis chiliophylla. Molecules, 24(8), 1468.

65. Li, D., Sun, C., Yang, J., Ma, X., Jiang, Y., Qiu, S., & Wang, G. (2019). Ionic Liquid-Microwave-Based Extraction of Biflavonoids from Selaginella sinensis. Molecules, 24(13), 2507.

66. Ndoile, M., & Van Heerden, F. (2018). Cytotoxic and antimalarial biflavonoids isolated from the aerial parts of Ochna serrulata (Hochst.) Walp. Tanzania Journal of Science, 44(3), 152-162.

67. Ibrahim, E. A., Desoukey, S. Y., Hadad, G. M., Salam, R. A., Ibrahim, A. K., Ahmed, S. A., ... & ElSohly, M. A. (2017). Analysis of cupressuflavone and amentoflavone from Cupressus sempervirens L. and its tissue cultured callus using HPLC-DAD method. Pharm Pharmacol Int J, 5(5), 174-180.

68. Sabudak, T., Ozturk, M., & Alpay, E. (2017). New Bioflavonoids from Solanum nigrum L. by Anticholinesterase and Anti-tyrosinase Activities-guided Fractionation. Records of Natural Products, 11(2), 130-140.

69. Shim, S. Y., Lee, S. G., & Lee, M. (2018). Biflavonoids isolated from Selaginella tamariscina and their anti-inflammatory activities via ERK 1/2 signaling. Molecules, 23(4), 926.

70. Mountessou, B. Y. G., Tchamgoue, J., Dzoyem, J. P., Tchuenguem, R. T., Surup, F., Choudhary, M. I., ... & Kouam, S. F. (2018). Two xanthones and two rotameric (3⟶ 8) biflavonoids from the Cameroonian medicinal plant Allanblackia floribunda Oliv.(Guttiferae). Tetrahedron Letters, 59(52), 4545-4550.

71. Shou, J. W., Zhang, R. R., Wu, H. Y., Xia, X., Nie, H., Jiang, R. W., & Shaw, P. C. (2018). Isolation of novel biflavonoids from Cardiocrinum giganteum seeds and characterization of their antitussive activities. Journal of ethnopharmacology, 222, 171-176.

72. Ndoile, M. M., & Van Heerden, F. R. (2018). Antimalarial Biflavonoids from the Roots of Ochna serrulata (Hochst.) Walp. International Research Journal of Pure and Applied Chemistry, 16, 1-9. https://doi.org/10.9734/IRJPAC/2018/42440

73. Al Groshi, A., Jasim, H. A., Evans, A. R., Ismail, F. M., Dempster, N. M., Nahar, L., & Sarker, S. D. (2019). Growth inhibitory activity of biflavonoids and diterpenoids from the leaves of the Libyan Juniperus phoenicea against human cancer cells. Phytotherapy Research, 33(8), 2075-2082.

74. Wagner, H., & Farkas, L. (1975). Synthesis of flavonoids. In The Flavonoids (pp. 127-213). Springer, Boston, MA.

75. Muller, D., & Fleury, J. P. (1991). A new strategy for the synthesis of biflavonoids via arylboronic acids. Tetrahedron letters, 32(20), 2229-2232.

76. Ali, S. M., & Ilyas, M. (1986). Biomimetic approach to biflavonoids: Oxidative coupling of 2'-hydroxychalcones with iodine in alkaline methanol. The Journal of Organic Chemistry, 51(26), 5415-5417.

77. Lin, Y. M., Flavin, M. T., Cassidy, C. S., Mar, A., & Chen, F. C. (2001). Biflavonoids as novel antituberculosis agents. Bioorganic & medicinal chemistry letters, 11(16), 2101-2104.

78. Riswanto, F. D., Rawa, M. S., Murugaiyah, V., Salin, N. H., Istyastono, E. P., Hariono, M., & Wahab, H. A. (2019). Anti-Cholinesterase Activity of Chalcone Derivatives: Synthesis, In Vitro Assay and Molecular Docking Study. Medicinal Chemistry (Shariqah (United Arab Emirates)).

79. Imran, S., Taha, M., Ismail, N. H., Kashif, S. M., Rahim, F., Jamil, W., ... & Wahab, H. (2015). Synthesis of novel flavone hydrazones: In-vitro evaluation of α-glucosidase inhibition, QSAR analysis and docking studies. European Journal of Medicinal Chemistry, 105, 156-170.

80. Kim, S. S., Vo, V. A., & Park, H. (2014). Synthesis of Ochnaflavone and Its Inhibitory Activity on PGE 2 Production. Bulletin of the Korean Chemical Society, 35(11), 3219-3223.

81. Sagrera, G., & Seoane, G. (2010). Total Synthesis of 3′, 3‴-Binaringenin and Related Biflavonoids. Synthesis, 2010(16), 2776-2786.

82. Nadirov, R. K., Nadirov, K. S., Esimova, A. M., & Nadirova, Z. K. (2014). Electrochemical synthesis of amino derivatives of biflavonoids. Chemistry of Natural Compounds, 50(4), 735-736.

83. Sum, T. H., Sum, T. J., Collins, S., Galloway, W. R., Twigg, D. G., Hollfelder, F., & Spring, D. R. (2017). Divergent synthesis of biflavonoids yields novel inhibitors of the aggregation of amyloid β (1–42). Organic & Biomolecular Chemistry, 15(21), 4554-4570.

84. Sum, T. J., Sum, T. H., Galloway, W. R., Twigg, D. G., Ciardiello, J. J., & Spring, D. R. (2018). Synthesis of structurally diverse biflavonoids. Tetrahedron, 74(38), 5089-5101.

85. Soto, M., Soengas, R. G., Silva, A. M., Gotor-Fernández, V., & Rodríguez-Solla, H. (2019). Temperature-Controlled Stereodivergent Synthesis of 2, 2′-Biflavanones Promoted by Samarium Diiodide. Chemistry–A European Journal, 25(57), 13104-13108.

86. Xu, K., Yang, C., Xu, Y., Li, D., Bao, S., Zou, Z., ... & Yu, X. (2020). Selective geranylation of biflavonoids by Aspergillus terreus aromatic prenyltransferase (AtaPT). Organic & Biomolecular Chemistry, 18(1), 28-31.

87. Anand, K., Ziebuhr, J., Wadhwani, P., Mesters, J. R., & Hilgenfeld, R. (2003). Coronavirus main proteinase (3CLpro) structure: basis for design of anti-SARS drugs. Science, 300(5626), 1763-1767.

88. Grum-Tokars, V., Ratia, K., Begaye, A., Baker, S. C., & Mesecar, A. D. (2008). Evaluating the 3C-like protease activity of SARS-Coronavirus: recommendations for standardized assays for drug discovery. Virus research, 133(1), 63-73.

89. Tian, X., Lu, G., Gao, F., Peng, H., Feng, Y., Ma, G., ... & Gao, G. F. (2009). Structure and cleavage specificity of the chymotrypsin-like serine protease (3CLSP/nsp4) of porcine reproductive and respiratory syndrome virus (PRRSV). Journal of molecular biology, 392(4), 977-993.

90. Kiemer, L., Lund, O., Brunak, S., & Blom, N. (2004). Coronavirus 3CL pro proteinase cleavage sites: Possible relevance to SARS virus pathology. BMC bioinformatics, 5(1), 72.

91. Thiel, V., Ivanov, K. A., Putics, A., Hertzig, T., Schelle, B., Bayer, S., ... & Gorbalenya, A. E. (2003). Mechanisms and enzymes involved in SARS coronavirus genome expression. Journal of General Virology, 84(9), 2305-2315.

92. Alamri, M. A., Tahir Ul Qamar, M., Mirza, M. U., Bhadane, R., Alqahtani, S. M., Muneer, I., ... & Salo-Ahen, O. M. (2020). Pharmacoinformatics and molecular dynamics simulation studies reveal potential covalent and FDA-approved inhibitors of SARS-CoV-2 main protease 3CLpro. Journal of Biomolecular Structure and Dynamics, 1-13.

93. Ghosh, A. K., Brindisi, M., Shahabi, D., Chapman, M. E., & Mesecar, A. D. (2020). Drug Development and Medicinal Chemistry Efforts toward SARS-Coronavirus and Covid-19 Therapeutics. ChemMedChem. https://doi.org/10.1002/cmdc.202000223 [Epub ahead of print]

94. Mesecar, A.D., A taxonomically-driven approach to development of potent, broad-spectrum inhibitors of coronavirus main protease including SARS-CoV-2 (COVID-19), http://www.rcsb.org/structure/6W63; 2020 (accessed 24 October 2020)

95. Stoermer, M. (2020). Homology Models of Coronavirus 2019-nCoV 3CLpro Protease.

96. Jin, Z., Du, X., Xu, Y., Deng, Y., Liu, M., Zhao, Y., ... & Duan, Y. (2020). Structure of M pro from SARS-CoV-2 and discovery of its inhibitors. Nature, 582, 289-293. https://doi.org/10.1038/s41586-020-2223-y

97. Zhang, L., Lin, D., Sun, X., Curth, U., Drosten, C., Sauerhering, L., ... & Hilgenfeld, R. (2020). Crystal structure of SARS-CoV-2 main protease provides a basis for design of improved α-ketoamide inhibitors. Science, 368(6489), 409-412.

98. Yang, H., Yang, M., Ding, Y., Liu, Y., Lou, Z., Zhou, Z., ... & Gao, G. F. (2003). The crystal structures of severe acute respiratory syndrome virus main protease and its complex with an inhibitor. Proceedings of the National Academy of Sciences, 100(23), 13190-13195.

99. Wang, F., Chen, C., Tan, W., Yang, K., & Yang, H. (2016). Structure of main protease from human coronavirus NL63: insights for wide spectrum anti-coronavirus drug design. Scientific reports, 6, 22677.

100. Acharya, A., Agarwal, R., Baker, M., Baudry, J., Bhowmik, D., Boehm, S., ... & Demerdash, O. (2020). Supercomputer-Based Ensemble Docking Drug Discovery Pipeline with Application to Covid-19. ChemRxiv, Preprint. https://doi.org/10.26434/chemrxiv.12725465.v1

101. Su, H. X., Yao, S., Zhao, W. F., Li, M. J., Zhang, L. K., Ye, Y., ... & Xu, Y. C. (2020). Identification of a novel inhibitor of SARS-CoV-2 3CLpro. published online, 10.

102. Ma, C., Sacco, M. D., Hurst, B., Townsend, J. A., Hu, Y., Szeto, T., ... & Wang, J. (2020). Boceprevir, GC-376, and calpain inhibitors II, XII inhibit SARS-CoV-2 viral replication by targeting the viral main protease. Cell Res 30, 678–692 (2020). https://doi.org/10.1038/s41422-020-0356-z

103. Mesecar, A.D. A taxonomically-driven approach to development of potent, broad-spectrum inhibitors of coronavirus main protease including SARS-CoV-2 (COVID-19), http://www.rcsb.org/structure/6W63 ; 2020 (accessed 24 October 2020).

104. Jin, Z., Zhao, Y., Sun, Y., Zhang, B., Wang, H., Wu, Y., ... & Duan, Y. (2020). Structural basis for the inhibition of SARS-CoV-2 main protease by antineoplastic drug carmofur. Nature structural & molecular biology, 27(6), 529-532.

105. Fearon, D., Owen, C.D., Douangamath, A., Lukacik, P., Powell, A.J., Strain-Damerell, C.M., ... & von Delft, F., PanDDA analysis group deposition SARS-CoV-2 main protease fragment screen, http://www.rcsb.org/structure/5RHF; 2020 (accessed 24 October 2020).

106. Kneller, D.W., Phillips, G., O'Neill, H.M., Jedrzejczak, R., Stols, L., Langan, P., ... & Coates, L., Kovalevsky, A., Structural plasticity of SARS-CoV-2 3CL Mproactive site cavity revealed by room temperature X-ray crystallographyl http://www.rcsb.org/structure/6WQF; 2020 (accessed 24 October 2020).

107. Kneller, D.W., Phillips, G., O'Neill, H.M., Tan, K., Joachimiak, A., Coates, L., Kovalevsky, A., Room temperature X-ray crystallography reveals catalytic cysteine in the SARS-CoV-2 3CL Mpro is highly reactive: Insights for enzyme mechanism and drug design, http://www.rcsb.org/structure/6XB1; 2020 (accessed 24 October 2020).

108. Wang, H., He, S., Deng, W., Zhang, Y., Li, G., Sun, J., Zhao, W... & Shang, L., Comprehensive Insights into the Catalytic Mechanism of Middle East Respiratory Syndrome 3C-Like Protease and Severe Acute Respiratory Syndrome 3C-Like Protease, http://www.rcsb.org/structure/6LO0; 2020 (accessed 24 October 2020).

109. Tan, K., Maltseva, N.I., Welk, L.F., Jedrzejczak, R.P., Joachimiak, A., The crystal structure of 3CL MainPro of SARS-CoV-2 with de-oxidized C145, http://www.rcsb.org/structure/7JFQ; 2020 (accessed 24 October 2020).

110. Tan, K., Maltseva, N.I., Welk, L.F., Jedrzejczak, R.P., Coates, L., Kovalevskyi, A.Y., Joachimiak, A., The crystal structure of 3CL MainPro of SARS-CoV-2 with oxidized Cys145 (Sulfenic acid cysteine), http://www.rcsb.org/structure/6XKF; 2020 (accessed 24 October 2020)

111. Tan, K., Maltseva, N.I., Welk, L.F., Jedrzejczak, R.P., Coates, L., Kovalevsky, A., Joachimiak, A. The 1.28a crystal structure of 3cl mainpro of sars-cov-2 with oxidized c145 (sulfinic acid cysteine), http://www.rcsb.org/structure/6XKH; 2020 (accessed 24 October 2020)

112. Tan, K., Maltseva, N.I., Welk, L.F., Jedrzejczak, R.P., Joachimiak, A. The crystal structure of 3CL MainPro of SARS-CoV-2 with C145S mutation, http://www.rcsb.org/structure/6XOA; 2020 (accessed 24 October 2020).

113. Kneller, D.W., Phillips, G., Weiss, K.L., Pant, S., Zhang, Q., O'Neill, H. ... & Kovalevsky, A., Protonation states in SARS-CoV-2 main protease mapped by neutron crystallography http://www.rcsb.org/structure/7JUN; 2020 (accessed 24 October 2020).

114. de Oliveira, R.R., Nascimento, A.F.Z., Zeri, A.C.M., Trivella, D.B.B., SARS-CoV-2 3CL protease crystallized under reducing conditions, https://www.rcsb.org/structure/7jr3 ; 2020 (accessed 24 October 2020).

115. Nascimento, A.F.Z., de Oliveira, R.R., Zeri, A.C.M., Trivella, D.B.B., SARS-CoV-2 3CL protease with alternative conformation of the active site promoted by methylene-bridged cysteine and lysine residues, http://www.rcsb.org/structure/7JR4; 2020 (accessed 24 October 2020).

116. Kneller, D.W., Phillips, G., O'Neill, H.M., Tan, K., Joachimiak, A., Coates, L., Kovalevsky, A. Room temperature X-ray crystallography reveals oxidation and reactivity of cysteine residues in SARS-CoV-2 3CL Mpro: Insights for enzyme mechanism and drug design, http://www.rcsb.org/structure/6XHU ; 2020 (accessed 24 October 2020).

117. Kneller, D.W., Galanie, S., Phillips, G., O'Neill, H.M., Coates, L., Kovalevsky, A. Extreme malleability of the SARS-CoV-2 3CL Mpro active site cavity facilitates binding of clinical antivirals: Prospects for repurposing existing drugs and ramifications for inhibitor design, http://www.rcsb.org/structure/6XQT ; 2020 (accessed 24 October 2020).

118. Rathnayake, A.D., Zheng, J., Kim, Y., Perera, K.D., Mackin, S., Meyerholz, D.K., Kashipathy, M.M., ... & Chang, K.O., 3C-like protease inhibitors block coronavirus replication in vitro and improve survival in MERS-CoV-infected mice, http://www.rcsb.org/structure/6W2A; 2020 (accessed 24 October 2020).

119. Vuong, W., Khan, M.B., Fischer, C., Arutyunova, E., Lamer, T., Shields, J. ... & McKay, R.T., van Belkum, M.J., Joyce, M.A., Young, H.S., Tyrrell, D.L., Vederas, J.C., Lemieux, M.J., Feline coronavirus drug inhibits the main protease of SARS-CoV-2 and blocks virus replication, http://www.rcsb.org/structure/6WTK; 2020 (accessed 24 October 2020).

120. Ma, C., Sacco, M., Chen, Y., Wang, J., Crystal structure of the SARS-CoV-2 (COVID-19) main protease in complex with inhibitor UAW247, http://www.rcsb.org/structure/6XBH ; 2020 (accessed 24 October 2020).

121. Ma, C., Sacco, M., Chen, Y., Wang, J., Crystal structure of the SARS-CoV-2 (COVID-19) main protease in complex with inhibitor, http://www.rcsb.org/structure/6XBG ; 2020 (accessed 24 October 2020).

122. Sacco, M., Chen, Y., Ma, C., Crystal structure of the SARS-CoV-2 (COVID-19) main protease in complex with UAW243, http://www.rcsb.org/structure/6XFN ; 2020 (accessed 24 October 2020).

123. Tan, K., Maltseva, N.I., Welk, L.F., Jedrzejczak, R.P., Joachimiak, A., The crystal structure of SARS-CoV-2 Main Protease in complex with masitinib, http://www.rcsb.org/structure/7JU7 ; 2020 (accessed 24 October 2020).

124. Zhu, L., Hilgenfeld, R., Crystal structures of SARS-Cov main protease complexed with a series of unsaturated esters, http://www.rcsb.org/structure/3SZN ; 2020 (accessed 24 October 2020).

125. Zhu, L., George, S., Schmidt, M.F., Al-Gharabli, S.I., Rademann, J., Hilgenfeld, R., Peptide aldehyde inhibitors challenge the substrate specificity of the SARS-coronavirus main protease, http://www.rcsb.org/structure/3SNE ; 2020 (accessed 24 October 2020).

126. Ma, C., Sacco, M., Chen, Y., Wang, J., Crystal structure of the SARS-CoV-2 (COVID-19) main protease in complex with inhibitor UAW248, http://www.rcsb.org/structure/6XBI ; 2020 (accessed 24 October 2020).

127. Hoffman, R.L., Kania, R.S., Brothers, M.A., Davies, J.F., Ferre, R.A., Gajiwala, K.S., He, M., Hogan, R.J., Kozminski, K., Li, L.Y., Lockner, J.W., Lou, J., Marra, M.T., Mitchell, L.J., Murray, B.W., Nieman, J.A., Noell, S., Planken, S.P., Rowe, T., Ryan, K., Smith, G.J., Solowiej, J.E., Steppan, C.M., Taggart, B., The Discovery of Ketone-Based Covalent Inhibitors of Coronavirus 3CL Proteases for the Potential Therapeutic Treatment of COVID-19, http://www.rcsb.org/structure/6XHO ; 2020 (accessed 24 October 2020).

128. Sacco, M., Chen, Y., Ma, C. Crystal structure of the SARS-CoV-2 (COVID-19) main protease in complex with UAW241, http://www.rcsb.org/structure/6XA4 ; 2020 (accessed 24 October 2020).

129. Zhang, L., Lin, D., Sun, X., Curth, U., Drosten, C., Sauerhering, L., Becker, S., Rox, K., Hilgenfeld, R., Crystal structure of SARS-CoV-2 main protease provides a basis for design of improved alpha-ketoamide inhibitors, http://www.rcsb.org/structure/6Y2E ; 2020 (accessed 24 October 2020).

130. Hattori, S.I., Higashi-Kuwata, N., Hayashi, H., Allu, R.S., Das, D., Takamune, N., Kishimoto, N., Takamatsu, Y., Bulut, H., Misumi, S., Ghosh, A.K., Mitsuya, H., A SARS-CoV-2's Main Protease-targeting Small-Compound GRL-2420 Completely Blocks the Infectivity and

Cytopathicity of SARS-CoV-2, http://www.rcsb.org/structure/7JKV ; 2020 (accessed 24 October 2020).

131. Schmidt, M., Malla, T., SARS cov-2 main protease 3clpro, room temperature, damage free xfel monoclinic structure, http://www.rcsb.org/structure/7JVZ ; 2020 (accessed 24 October 2020).

132. Littler, D.R., Gully, B.S., Colson, R.N., Rossjohn, J. Crystal Structure of the SARS-CoV-2 Non-structural Protein 9, Nsp9, http://www.rcsb.org/structure/6W9Q ; 2020 (accessed 24 October 2020).

133. Fu, L.F., Crystal structure of the 2019-nCoV main protease complexed with GC376, http://www.rcsb.org/structure/7BRR ; 2020 (accessed 24 October 2020).

134. Fu, L.F., Crystal structure of the 2019-nCoV main protease, http://www.rcsb.org/structure/7BRO ; 2020 (accessed 24 October 2020).

135. Fu, L.F., Crystal structure of the 2019-nCoV main protease complexed with Boceprevir, http://www.rcsb.org/structure/7BRP ; 2020 (accessed 24 October 2020).

136. Zhou, X.L., Zhong, F.L., Lin, C., Hu, X.H., Zhou, H., Wang, Q.S., Li, J., Zhang, J., The crystal structure of COVID-19 main protease in the apo state, http://www.rcsb.org/structure/7C2Q ; 2020 (accessed 24 October 2020).

137. Kuo, C.J., Shie, J.J., Lin, C.H., Lin, Y.L., Hsieh, M.C., Lee, C.C., Chang, S.Y., Wang, A.H.J., Liang, P.H., Complex Structures and Cellular Activities of the Potent SARS-CoV-2 3CLpro Inhibitors Guiding Drug Discovery Against COVID-19, http://www.rcsb.org/structure/7C8T ; 2020 (accessed 24 October 2020).

138. Kneller, D.W., Coates, L., Kovalevsky, A., Structure of the complex between the SARS-CoV-2 Main Protease and Leupeptin, http://www.rcsb.org/structure/6XCH ; 2020 (accessed 24 October 2020).

139. Ye, G., Wang, X., Tong, X., Shi, Y., Fu, Z.F., Peng, G., Structural Basis for Inhibiting Porcine Epidemic Diarrhea Virus Replication with the 3C-Like Protease Inhibitor GC376, http://www.rcsb.org/structure/6L70 ; 2020 (accessed 24 October 2020).

140. Zhang, L., Lin, D., Kusov, Y., Nian, Y., Ma, Q., Wang, J., von Brunn, A., Leyssen, P., Lanko, K., Neyts, J., de Wilde, A.H., Snijder, E.J., Liu, H., Hilgenfeld, R., Alpha-ketoamides as broad-spectrum inhibitors of coronavirus and enterovirus replication Structure-based design, synthesis, and activity assessment, http://www.rcsb.org/structure/6FV1 ; 2020 (accessed 24 October 2020).

141. Qiao, J.X., Zeng, R., Li, Y.S., Wang, Y.F., Lei, J., Yang, S.Y., Crystal structure of SARS-CoV-2 main protease in complex with MI-23, http://www.rcsb.org/structure/7D3I ; 2020 (accessed 24 October 2020).
142. Fu, L.F., Feng, Y., Qi, J.X., Crystal structure of SARS-Cov-2 main protease with narlaprevir, http://www.rcsb.org/structure/7D1O ; 2020 (accessed 24 October 2020).
143. Qiao, J.X., Zeng, R., Wang, Y.F., Li, Y.S., Yao, R., Zhou, Y.L., Chen, P., Lei, J., Yang, S.Y., Crystal structure of the SARS-CoV-2 main protease in complex with Telaprevir, http://www.rcsb.org/structure/7C7P ; 2020 (accessed 24 October 2020).
144. Qiao, J.X., Zeng, R., Wang, Y.F., Li, Y.S., Yao, R., Liu, J.M., Zhou, Y.L., Chen, P., Lei, J., Yang, S.Y., Crystal structure of the SARS-CoV-2 main protease in complex with Boceprevir (space group P212121), http://www.rcsb.org/structure/7COM ; 2020 (accessed 24 October 2020).
145. Oerlemans, R., Wang, W., Lunev, S., Domling, A., Groves, M.R., Crystal structure of SARS CoV2 main protease in complex with inhibitor Boceprevir, http://www.rcsb.org/structure/6ZRU ; 2020 (accessed 24 October 2020).
146. Oerlemans, R., Wang, W., Lunev, S., Domling, A., Groves, M.R., Crystal structure of SARS CoV2 main protease in complex with inhibitor Telaprevir, http://www.rcsb.org/structure/6ZRT ; 2020 (accessed 24 October 2020).
147. Mohan, K., Ueda, G., Kim, A.R., Jude, K.M., Fallas, J.A., Guo, Y., Hafer, M., Miao, Y., Saxton, R.A., Piehler, J., Sankaran, V.G., Baker, D., Garcia, K.C., Topological control of cytokine receptor signaling induces differential effects in hematopoiesis, http://www.rcsb.org/structure/6MOK ; 2020 (accessed 24 October 2020).
148. Dai, W., Zhang, B., Jiang, X.M., Su, H., Li, J., Zhao, Y., Xie, X., Jin, Z., Peng, J., Liu, F., Li, C., Li, Y., Bai, F., Wang, H., Cheng, X., Cen, X., Hu, S., Yang, X., Wang, J., Liu, X., Xiao, G., Jiang, H., Rao, Z., Zhang, L.K., Xu, Y., Yang, H., Liu, H., Structure-based design of antiviral drug candidates targeting the SARS-CoV-2 main protease, http://www.rcsb.org/structure/6LZE ; 2020 (accessed 24 October 2020).
149. Fu, L., Feng, Y., Crystal structure of the SARS-CoV-2 main protease complexed with Boceprevir, http://www.rcsb.org/structure/7C6S ; 2020 (accessed 24 October 2020).
150. Qiao, J.X., Zeng, R., Liu, X.L., Nan, J.S., Wang, Y.F., Li, Y.S., Lei, J., Yang, S.Y., Crystal structure of the SARS-CoV-2 main protease in complex with INZ-1, http://www.rcsb.org/structure/7CX9 ; 2020 (accessed 24 October 2020).

151. Gontijo, V. S., Judice, W. A., Codonho, B., Pereira, I. O., Assis, D. M., Januário, J. P., ... & Junior, C. V. (2012). Leishmanicidal, antiproteolytic and antioxidant evaluation of natural biflavonoids isolated from Garcinia brasiliensis and their semisynthetic derivatives. European journal of medicinal chemistry, 58, 613-623.

152. Gontijo, V. S., Januário, J. P., de Souza Júdice, W. A., Antunes, A. A., Cabral, I. R., Assis, D. M., ... & dos Santos, M. H. (2015). Morelloflavone and its semisynthetic derivatives as potential novel inhibitors of cysteine and serine proteases. Journal of Medicinal Plants Research, 9(13), 426-434.

153. Assis, D. M., Gontijo, V. S., de Oliveira Pereira, I., Santos, J. A. N., Camps, I., Nagem, T. J., ... & Doriguetto, A. C. (2013). Inhibition of cysteine proteases by a natural biflavone: behavioral evaluation of fukugetin as papain and cruzain inhibitor. Journal of Enzyme Inhibition and Medicinal Chemistry, 28(4), 661-670.

154. Fazio, N. F., Russell, M. H., Flinders, S. M., Gardner, C. J., Webster, J. B., & Hansen, M. D. (2020). A natural product biflavonoid scaffold with anti-tryptase activity. Naunyn-Schmiedeberg's Archives of Pharmacology, 1-9. https://doi.org/10.1007/s00210-020-01959-2

155. Lee, C. W., Choi, H. J., Kim, H. S., Kim, D. H., Chang, I. S., Moon, H. T., ... & Woo, E. R. (2008). Biflavonoids isolated from Selaginella tamariscina regulate the expression of matrix metalloproteinase in human skin fibroblasts. Bioorganic & medicinal chemistry, 16(2), 732-738.

156. Yap, B. K., Lee, C. Y., Choi, S. B., Kamarulzaman, E. E., Hariono, M., & Wahab, H. A. (2019). In Silico Identification of Novel Inhibitors. 3. 761-779.

157. Sulaiman, S. N., Hariono, M., Salleh, H. M., Chong, S. L., Yee, L. S., Zahari, A., ... & Awang, K. (2019). Chemical Constituents From Endiandra kingiana (Lauraceae) as Potential Inhibitors for Dengue Type 2 NS2B/NS3 Serine Protease and its Molecular Docking. Natural Product Communications, 14(9), 1934578X19861014.

158. El Sahili, A., & Lescar, J. (2017). Dengue virus non-structural protein 5. Viruses, 9(4), 91.

159. Sahin, A. R., Erdogan, A., Agaoglu, P. M., Dineri, Y., Cakirci, A. Y., Senel, M. E., ... & Tasdogan, A. M. (2020). 2019 Novel Coronavirus (COVID-19) Outbreak: A Review of the Current Literature. EJMO, 4(1), 1-7.

160. Di, L. (2015). Strategic approaches to optimizing peptide ADME properties. The AAPS journal, 17(1), 134-143.

161. Janani Swaminathan & Carsten Ehrhardt (2012) Liposomal delivery of proteins and peptides, Expert Opinion on Drug Delivery, 9:12, 1489-1503, https://doi.org/10.1517/17425247.2012.735658

162. Mozafari, M. R. (2005). Liposomes: an overview of manufacturing techniques. Cellular and Molecular Biology Letters, 10(4), 711.

163. Tajabadi, F. M., Campitelli, M. R. & Quinn, R. J. Scaffold Flatness: Reversing the Trend. Springer Sci. Rev. 1, 141–151 (2013).

164. Hariono, M., Yuliani, S. H., Istyastono, E. P., Riswanto, F. D., & Adhipandito, C. F. (2018). Matrix metalloproteinase 9 (MMP9) in wound healing of diabetic foot ulcer: Molecular target and structure-based drug design. Wound Medicine, 22, 1-13.

165. Istyastono, E. P., Yuniarti, N. U. N. U. N. G., Hariono, M., Yuliani, S. H., & Riswanto, F. D. O. (2017). Binary quantitative structure-activity relationship analysis in retrospective structure based virtual screening campaigns targeting estrogen receptor alpha. Asian Journal of Pharmaceutical and Clinical Sciences 10(12), 206-211.

Results in Chemistry will receive its first Impact Factor

Editorial Board <STMJournals@author.email.elsevier.com>

Wed 10/26/2022 2:10 PM

To: Yustina Sri Hartini <yustinahartini@usd.ac.id>

Dear Yustina Hartini,

We are delighted to inform you that the gold open access *Results in Chemistry*, in which you published '[Biflavonoid as potential 3-chymotrypsin-like protease (3CLpro) inhibitor of SARS-Coronavirus]', will receive its first Journal Impact Factor (JIF)* in June 2023.

The Journal Impact Factor will increase the visibility and reach of the publication and your work to a broader global research audience, making an even greater impact in our community.

This is Open Access Week, and we thank you very much for supporting the open sharing of knowledge. Your work has helped to advance open science in your field of research. We hope you will consider us for your next publication.

If you would like to read articles and insights from the journal and remind yourself of the submission process, please visit the journal homepage.

Yours sincerely,
Editorial Board of *Results in Chemistry*

*Source: Journal Citation Reports™ from Clarivate Analytics